ON A SPATIOTEMPORAL POPULATION DYNAMICS MODEL TO TRACK DENSITY AND AVERAGE MASS: APPLICATION TO BROWN SHRIMP (*FARFANTEPENAEUS AZTECUS*) IN GULF OF MEXICO

A Dissertation

by

BHEEMAIAH VEENA SHANKARA NARAYANA RAO

Submitted to the Office of Graduate and Professional Studies of
Texas A&M University
in partial fulfillment of the requirements for the degree of

DOCTOR OF PHILOSOPHY

Chair of Committee,	Jay R Walton
Co-Chair of Committee,	Masami Fujiwara
Committee Members,	Peter Howard
	Tom Vogel
Head of Department,	Emil Straube

December 2016

Major Subject: Mathematics

ABSTRACT

Structured population models have been used to model density of individuals over time and other factors such as age, mass, developmental stage and space. Mass is a particularly useful measure of condition of a population. For example, large individuals tend to reproduce more offspring and survive better than smaller ones. Traditional models of mass as a continuous structure parameter do not introduce a separate partial differential equation (PDE) for mass; rather they model the population as being subdivided into classes parameterized by mass and then number density is written as a function of spatial location, time and mass. Our approach to modeling mass dependent population dynamics introduces mass as a dependent variable. In particular, we developed a new PDE for mass where mass is a function of spatial location and time.

We constructed a spatiotemporal population dynamics model to track density and average mass of the population at location x and time t and the model will be called as density and mass model. Our model provides an insight into the identification of key processes (reproduction, growth, mortality) controlling populations over various space and time. We developed a finite difference scheme for the numerical solution to the system of PDEs arising from our modeling effort. Then the model is applied to brown shrimp in the Gulf of Mexico to understand their spatiotemporal dynamics of density and mass.

To derive a density and mass model, we start with conservation laws for biomass and number density. Then, we define average mass and derive the system of coupled parabolic and hyperbolic PDEs for spatial movement of individuals in a population. Then, birth, growth and death processes are added to derive the final system of PDEs to include spatial movements, birth, growth and death of individuals. Then, we impose fishing to some locations to investigate fishery yield.

Among the issues studied in the application of the general theory to brown shrimp in the Gulf of Mexico are: (1) investigate how the mobility of species affects the yield with multiple fishing zones and network of marine protected areas (MPAs), (2) test the efficacy of MPAs under multiple fishing zones, and (3) investigate how mass dependent mortality influences density and mass of a population. Calculating yield is critically important for helping the fishers to earn a better profit and keeping the population sustainable.

The results show that (1) to obtain a maximum sustainable biomass yield (MSBY), it is crucial to consider the speed or mobility of species under consideration before MPAs are designed, (2) when a network of MPAs are designed along the coastline, the fishing rate at MSBY increases with the number of marine protected areas and (3) small MPAs are very effective in producing a sustainable biomass yield for a low mobile species.

DEDICATION

This work is dedicated to my parents, Shankara Narayana Rao and Shakuntala.

ACKNOWLEDGEMENTS

First of all, I would like to express my sincere thanks to my advisor Professor Jay R.Walton for his continuous support, patience and encouragement. I feel honored to be advised by such an outstanding mathematician and generous mentor. All his guidance will be a great source for me to advance in my academic career. Working with him has been an enriching experience and I thank him for giving me this opportunity.

I would like to thank my co-advisor, Professor Masami Fujiwara, for his insightful suggestions and the guidance that he provided me during the course of my research. His classes on Population Dynamics and Marine Fisheries Management were very important for my research.

I am also grateful to Professors Peter Howard and Tom Vogel for serving on my dissertation committee and for providing me the valuable comments and suggestions to improve the quality of my dissertation.

I would like to thank all my professors at Texas A&M University with whom I took classes. I also wish to thank the Department of Mathematics at Texas A&M University for the wonderful research facility offered to me during last six years. I wish to thank Ms. Monique Stewart for all the help in completing the required paper works on time. I am also very appreciative of the financial support provided by the Department of Mathematics and the Texas Sea Grant (NA10OAR4170099).

I would also like to thank my friends - Emma, Sangin, Maya, Tina, Fahad, Jun, Srinivas - for their friendship and selflessly helping me whenever I needed. I would also like to acknowledge my thanks to Professor Dambaru Bhatta and his wife Bisruthi Bhatta from Edinburg, Texas, for their love and support throughout my graduate studies.

I would like to express my thanks to my husband Mallikarjun and my son Mahit for their unwavering love and support upon which the past 6 years of my life has been built. I would like to thank my parents, for their faith in me and allowing me to grow up into the person I am today. Also, I thank my siblings, brother's and sister in law - Lakshmi, Padmini, Ranga, Raju, Rajesh, Sindhu - for their unending encouragement and support.

And finally, thank you god for all your blessings to me.

NOMENCLATURE

BVP	Boundary Value Problem
FDM	Finite Difference Method
IVP	Initial Value Problem
ODE	Ordinary Differential Equation
PDE	Partial Differential Equation
TPWD	Texas Parks and Wildlife Department
NMFS	National Marine Fisheries Service
ICES	International Council for the Exploration of the Sea
FAO	Food and Agriculture Organization (United Nations)
NMFS	National Marine Fisheries Service
NOAA	National Oceanic and Atmospheric Administration
SERO	Southeast Regional Office

TABLE OF CONTENTS

LIST OF FIGURES

FIGURE Page

LIST OF TABLES

TABLE Page

1. INTRODUCTION

1.1 Structured Population Models

Structured population models are used for modeling changes in the density of individuals over time and other factors such as age, mass, developmental stage, and space. For example, the McKendrick partial differential equation (also called von Foerster partial differential equation) is written in the form

$$\frac{\partial P}{\partial t} + \frac{\partial P}{\partial a} + \mu(a)P = 0 \tag{1.1}$$

where $P = P(a, t)$ is the population density of age a at time t. It has been widely used in epidemiology and population study. In these models births are handled through a boundary condition with respect to age a variable,

$$P(0, t) = \int_0^{\omega} m(a, t)P(a, t)\, da \tag{1.2}$$

where $m(a, t)$ is the birth rate which varies with age and time, ω denotes the maximum attainable age. It is important to note that integral type boundary conditions involve a lot of data storage. Initial age distribution is given by,

$$P(a, 0) = P_0(a). \tag{1.3}$$

Here, time and age are independent variables, $\mu(a)$ is the instantaneous death rate for individuals of age a at time t. Instantaneous rates are the per capita rates.

Keyfitz and Keyfitz [34] discuss the solution of (1.1) and compare it to Thompson-Cole difference equation, Lotka's integral equation, and Leslie matrix. It has been shown that with small intervals of age and time all four forms of age structured model (two discrete and two continuous) are identical. Kot [37] discusses about each of these models and also makes a note of similarities. Each of the four models possesses: 1) a characteristic equation, 2) a dominant eigenvalue which helps to track population growth rate, and 3) a positive right eigenvector which leads to a stable age distribution [37].

The method of characteristics to solve the partial differential equation (1.1) subjected to conditions (1.2) and (1.3) leads to the Lotka's integral equation. The reader is directed to references [34,37] for the proof. In particular, the Lotka's integral equation involves a compact operator; as a consequence, it is characterized by a discrete spectrum of eigenvalues, and the solution can be expressed as a superposition of eigenfunctions [34]. It is necessary to note that, this is not true for a partial differential equation on an unbounded region, the boundary condition (1.2) has the remarkable property of making the problem compact. If the operator is compact, there exits a dominant eigenvalue λ such that $0 \leq \lambda' < \lambda$, that is, a dominant eigenvalue which is strictly larger in absolute values than any other eigenvalues. The corresponding right eigenvector is positive. The ecological application of eigenvalues and eigenvectors are discussed in [37].

However these forms can include only one dependent variable (population density) and two independent variables (time and age); but one might want to model a population with more than one dependent variable. Suppose we want to keep track of mass in addition to density and also want to keep track of time and space. Here density is the number of individuals per unit domain and mass means mass (weight) per individual. This is common in fishery management, for example. This incorporates four variables: two independent variables (time and space) and two dependent variables (density and mass). Here, we propose to develop a model for temporal change in population that utilizes two densities (number density and biomass density) as dependent variables. We call the model, a density and mass model.

A population's structure is very important in understanding its dynamics. For example, the performance of a population in two different locations might be very different if one group consisted of nearly all juveniles while the other group consisted of nearly all mature adults. Mass is a particularly useful measure of condition of a population. Furthermore, large individuals may reproduce more offspring than smaller ones. Figure 1.1 shows how size affects the reproduction of vermilion-rockfish and the data was obtained from NOAA Technical Report [41, 48]. Larger vermilion-rockfish produced 88% more offspring compared to smallest vermilion-rockfish. Difference in size between largest and the smallest was found to be around 9 inches, but this produced a huge difference in young individuals. In Figure 1.1, each offspring represents 100,000 young individuals. This example illustrates the importance of size structure.

Juvenile growth and mortality effects on white shrimp population dynamics were studied in [3]. It also indicates the importance of population structure. A population model to calculate the annual population growth rate R_y between two consecutive years y and $y+1$ was developed,

$$R_y = S_0\ S_1\ S_2\ S_3\ S_4\ f_4. \tag{1.4}$$

Here S_i is the survivor ship of stage i over the duration of time spent in that stage and f_4 is the annual per-capita fecundity. Life cycle of shrimp is divided into five stages: egg/larvae, early juveniles, late juveniles, bay sub-adult and offshore adult. Fecundity is the rate of production of offsping per adult. This model incorporates vital rates (growth, mortality, fecundity) for each life stage of shrimp and how juvenile growth and mortality rates affects the growth rate of entire stock has been explored. The

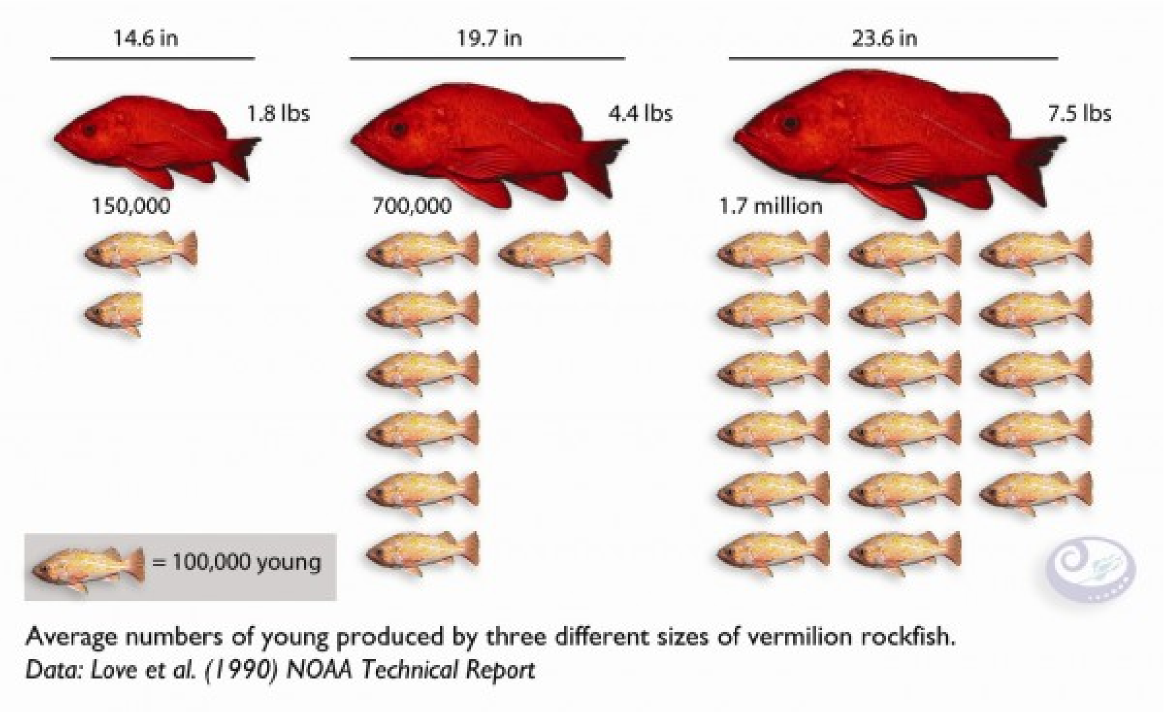

Figure 1.1: Vermilion-rockfish reproduction. Reprinted with permission from [41].

results suggest that changes in the juvenile growth and mortality rates had a greater impact on adult stock size compared to fishing pressure on the entire stock [3].

Unfortunately, their model omits any space variable. However, spatial distribution can be critically important because different fishery management strategies (e.g. catch control and effort control) are implemented among different locations. Catch (harvest) is the total number (or weight) of fish caught by fishing operations. Effort is the amount of time and fishing intensity used to harvest fish; effort units include gear size, boat size.

1.2 Traditional Model in Population Dynamics

The standard approach of modeling mass in population dynamics is to introduce it as a structure parameter subject to its own evolution law. The mass parameter can be modeled as being discrete, leading to compartmental type model or continuous, leading to partial differential equation. Mass as a continuous structure parameter within a spatially heterogenous population model is traditionally modeled through equations of the form

$$\frac{\partial n(t,x,w)}{\partial t} + \frac{\partial(\gamma(t,x,w)n(t,x,w))}{\partial w} = -\nabla.(n(t,x,w)\mathbf{v}(t,x,w)) - \delta(t,x,w), \tag{1.5}$$

in which n, w, γ and δ denote number density, mass, growth law and death law, respectively, and $\mathbf{v}$ is a velocity vector field modeling spatial transport. Births are handled through an initial condition with respect to the mass variable. Initial conditions are of the form

$$n(t, w_b) = \int_{w_b}^{\infty} \beta(t,w)n(t,w)\, dw \tag{1.6}$$

$$n(0,w) = n_0(w), \ \ \text{for } w_b \leq w, \tag{1.7}$$

where $\beta(t,w)$ is the fecundity for individuals with the mass 'w' and 'w_b' is the birth mass.

When mass is modeled as a structure parameter, the dimensionality of the partial differential equation (1.5) is increased by one over the corresponding model without mass structure. This is computationally expensive. An alternative approach is to introduce mass as a additional dependent variable. For this, we need to add an additional partial differential equation with the same space time dimensionality as the corresponding model without mass dependence. It is computationally less expensive to create a mass dependent population dynamics model from a mass independent one by adding mass as an additional dependent variable rather than as an additional independent one.

In a recent (May 5th 2016) article by TPWD News Media [80], Coastal Fisheries Division for TPWD decided to close state's shrimp season to shrimpers in Gulf contingent on sampling results of average size and density of brown shrimp. Every year, the Gulf of Mexico commercial shrimp season for both Texas and federal waters is closed for two months to give little shrimp time to grow to a larger and valuable size before being harvested. Despite of all these efforts to improve shrimp industry, Texas shrimpers are making very little profit these days. This calls for a better understanding of spatiotemporal dynamics of a population and thus modeling population abundance and mass of brown shrimp over different spatial and temporal scales makes it an exciting research opportunity.

1.3 A Brief Introduction to Ecology

Ecology is one among the many branches of Biology. The term Ecology was first defined by German zoologist Ernst Haeckel as "Haushaltslehre de Nature" which means the study of the economics of nature [40]. Literature survey helps us to know that there are different definitions of Ecology [24]. Four of the prevalent definitions will be listed in this discussion. The first of it is the Haeckelian form cited above. The second definition considers ecology to be the scientific study of the distribution and abundance of organisms [2]. The third definition was by American Biologist Eugene P. Odum who defined Ecology to be the study of nature and ecosystem. The fourth is the circular definition which says "a population is composed of a number of individuals which are connected to the rest of the population" [25]. Due to vast material and ever lasting difference of opinion in its definition, this subject can be classified into a wide variety of branches depending upon the level of complexity (low to high), organism under study (animals, plants, microbes), spatial scale under study (global, landscape). A few of them are listed here namely theoretical ecology, conservation ecology, behavioral ecology, marine ecology, population ecology, human ecology, evolutionary ecology, systems ecology. Despite the variation in the definition, there is a general agreement on the subject matter. In its most basic form, it can be grouped into study of abundance, environment, evolution, distribution of species.

While modeling a population one needs to make a note of amount of fluctuation in a population. Nisbet and Gurney discuss ecological and mathematical stability [59] and define ecologically stable population to be the one which is sustainable for more generations and when the population is not ecologically stable it is not sustainable for many generations. Estimating the mean time τ_E which drives the population extinct, helps to discuss ecological stability. However, for knowing the effect of a vital processes - birth, death, growth in a population, it is always good to define stability index η,

$$\eta = ln\ \tau_E. \tag{1.8}$$

It is important to note that stability index is defined in terms of logarithmic value of mean time because it is the order of magnitude which is used to understand effect of “stabilizing” [59]. In most of the realistic models in population dynamics, birth and death rates change with the density in a nonlinear fashion. It is customary that population dynamics models involve nonlinear equations of some type say: ODE, PDE, Difference Equation, Integro DE. Our interest lies in population ecology. Ecological research is distinctly interdisciplinary and mathematics have played an important role in the development of theoretical ecology [23, 54, 59].

1.4 Dissertation Outline

The rest of this dissertation is organized as follows: In Chapter 2, we discuss our approach of mass dependent population dynamics model and derive the density and mass model. Starting with conservation laws for biomass and number density, we define average mass (mass per individual) and derive the growth model. We add a spatial transport term to the system of ODEs derived and hence obtain the system of coupled nonlinear PDEs.

We consider a mass dependent transport coefficient in Chapter 3. Therefore the system of coupled nonlinear parabolic and hyperbolic PDE constructed in Chapter 2 yields a system of coupled nonlinear reaction diffusion-hyperbolic PDEs to track density and mass of a population at location x and time t.

We start with brief history of FDM in Chapter 4, we discuss how this method will be used for density and mass model. The density and average mass of a population is then the solution of a partial difference equation evaluated at a discrete point in space x and time t. In particular, we develop an explicit finite difference scheme for the numerical solution to the system of coupled nonlinear partial differential equations. This numerical method has been chosen because it is simple to implement, flexible in modeling so many processes and parameters in the model and also the explicit method speeds our computations.

In Chapter 5 we apply the density and mass model to Gulf of Mexico brown shrimp fishery. We examine three major aspects: 1) Marine protected areas (size/number of protected areas/fishing zones) 2) Instantaneous and Sustainable biomass yield 3) Mass dependent mortality and reproduction.

In the final Chapter 6, we give some concluding remarks and ideas for future work.

2. DERIVATION OF THE SPATIOTEMPORAL POPULATION DYNAMICS MODEL TO TRACK DENSITY AND MASS OF A POPULATION

2.1 Mass Dependent Population Dynamics Model

Our approach to introduce a measure of mass, besides a structure parameter model, is to track number density, $n(x,t)$, and biomass density, $\rho(x,t)$, of a population. We define number density $n(x,t)$ to be the number of individuals in a population per unit domain. In 1-D the domain is a unit length and in 2-D, domain is unit area. Biomass density $\rho(x,t)$ is defined as the total biomass per unit domain. We define the measure of mass through

$$w(x,t) = \frac{\rho(x,t)}{n(x,t)}, \tag{2.1}$$

which is the average mass per creature at location x at time t. While constructing any population dynamics model, it is necessary to write down the conservation laws. The beauty of conservation laws is that they allow for interactions between a system and the universe outside of the system, that is, they allow for growth, decline, immigration, emigration, accretion, ablation, etc. So we now look into brief history of these laws in the following Subsection.

2.1.1 Conservation Laws

The history of conservation laws dates back to the end of 18th-century when Antoine-Laurent de Lavoisier a French scientist and chemist was the first to introduce the law of conservation of mass. This means mass can be neither created nor destroyed in chemical reactions. This was a foundation for all different types of conservation laws used in today's contemporary scientific world [76]. Population models in ecology, epidemiology and mathematical biology may also involve the conservation law. But existence of general laws in these models are always debated. This is very important point to be noted while constructing models. Turchin makes a comment that none of the laws which he discusses in his paper [82] are new, rather ecologists have been using this law and this dates back to the days of Lotka, Volterra and Gause [37]. In simple words, conservation law means " What goes in must come out". The number of individuals in a population can change due to four factors: birth, death, immigration and emigration. In a closed system, we disregard immigration and emigration. So we now start by writing the law of conservation: The rate of change of number of individuals in a population can be represented mathematically by the equation

$$\frac{dN}{dt} = B(N) - D(N), \tag{2.2}$$

where N is the total number of individuals in a population, $B(N)$ is the birth rate or the reproduction rate, (that is, the rate at which individuals are born into the population) and $D(N)$ is the death rate, (that is, the rate which brings down the population due to death). This law will be used in the derivation of density and mass model which will be discussed in the following Subsection.

2.1.2 Density and Mass Conservation

In a continuum approach to modeling a population with spatial effects, movement must be understood at the population level. That is, population density spreads throughout a region rather than the motion of members of the population. Such a population spread is often modeled through a diffusive process. A convenient way to include this effect is through introduction of a velocity function, $\mathbf{v}(t, x)$ for a population defined on region R which describes movement of the population around the region.

In particular, a population density $u(t, x)$ spread is said to be diffusive if the velocity vector of the population density is proportional to the negative density gradient, that is, $\mathbf{v}(t, x)$ can be constitutively written as

$$u(t, x)\mathbf{v}(t, x) = -\mu \nabla u(t, x) \tag{2.3}$$

where μ is the diffusion coefficient. Thus, the constitutive choice in expression (2.3) means that the population move in the direction of maximum decrease of number of individuals [84].

Tracking both number $n(x, t)$ and biomass $\rho(x, t)$ densities, and the assumption of diffusive transport lead to two natural choices for the velocity vector field $\mathbf{v}$, namely

$$\mathbf{v} = -\mu \frac{\nabla \rho}{\rho} \tag{2.4}$$

or

$$\mathbf{v} = -\mu \frac{\nabla n}{n} \tag{2.5}$$

where μ denotes the transport coefficient.

One might model the number density $n(x, t)$ as follows

$$\frac{\partial n}{\partial t} + \nabla.(n\mathbf{v}) + (D - B) = 0. \tag{2.6}$$

This equation says how number density changes due to diffusive transport, birth and death. In addition to the birth and death rates, growth of an individual affects the biomass density. Let G be the growth rate function, that is, the rate at which an individual grows which accounts for the change in the average mass. The conservation law for biomass density and biomass $\rho(x, t)$ is given by

$$\frac{\partial \rho}{\partial t} + \nabla.(\rho\mathbf{v}) + w(D - B) - nG = 0, \tag{2.7}$$

where D is the death rate, B is the birth rate and G is the growth rate functions. Equation (2.7) is the conservation law for biomass density and this says how biomass evolves due to transport, birth, death and growth.

2.2 Density and Mass Model

Rewriting definition of average mass (2.1), we get an expression for biomass density $\rho(x,t)$,

$$\rho(x,t) = n(x,t)\ w(x,t). \tag{2.8}$$

Now differentiate (2.8) with respect to t,

$$\rho'(x,t) = n'(x,t)w(x,t) + n(x,t)w'(x,t). \tag{2.9}$$

Using the equations (2.8),(2.9) in (2.7) and (2.6), we get

$$n'w + nw' + (n\nabla w + w\nabla n).\mathbf{v} + wn(\nabla.\mathbf{v}) + w(D - B) = nG \tag{2.10}$$

$$n' = -(D - B) - (\nabla n).\mathbf{v} - n\nabla.\mathbf{v} \tag{2.11}$$

By eliminating n' in the above two equations (2.10) and (2.11), we have

$$\begin{multline} - w(D - B) - w(\nabla n).\mathbf{v} - wn(\nabla.\mathbf{v}) + \\ nw' + (n\nabla w + w\nabla n).\mathbf{v} + wn(\nabla.\mathbf{v}) + w(D - B) = nG. \end{multline} \tag{2.12}$$

After simplifying the above equation, we get the following PDE for average mass

$$w' + \mathbf{v}.\nabla w = G. \tag{2.13}$$

This equation says how average mass of a population changes due to movement and growth. We now list all the four fundamental number density - average mass - biomass density relations derived above,

$$\rho' + \nabla.(\rho\mathbf{v}) + w(D - B) = nG \tag{2.14}$$

$$n' + \nabla.(n\mathbf{v}) + (D - B) = 0 \tag{2.15}$$

$$w' + \mathbf{v}.\nabla w = G \tag{2.16}$$

$$w = \frac{\rho}{n}. \tag{2.17}$$

We are interested in tracking number density and average mass of a population. Apparently, our choice for velocity vector $\mathbf{v}$, would be

$$\mathbf{v} = -\frac{\mu}{n}\nabla n. \tag{2.18}$$

Then we rewrite (2.15) and (2.16) as

$$n' - \nabla.(\mu\nabla n) = B - D \tag{2.19}$$

$$w' + \nabla w.(-\frac{\mu}{n}\nabla n) = G. \tag{2.20}$$

Further, taking μ to be a constant results in

$$n' - \mu\Delta n = B - D \tag{2.21}$$

$$w' - \mu(\frac{\nabla n.\nabla w}{n}) = G. \tag{2.22}$$

Henceforth, we refer to number density and average mass as density and mass respectively. Both of these terms still retain their definitions: density is the number of individuals per unit domain and mass means mass per individual (average mass). The above system of equations, although obtained after several simplifying assumptions, are still very complicated to analyse. Equation (2.21) is a parabolic partial differential equation whereas equation (2.22) is a first order hyperbolic partial differential equation. Here B, D and G denote the birth, death and growth processes, which are functions of density n and mass w. Parabolic and hyperbolic PDEs have different qualitative properties. Setting $B - D = 0$, (2.21) becomes the classical diffusion equation, which sets as an example for heat conduction model based upon Fourier's law of heat flow. Regardless of the initial state, solutions to the heat equation are infinitely smooth and converge to a spatially uniform distribution as $t \to \infty$.

Now when $G = 0$, equation (2.22) becomes a first order homogeneous hyperbolic PDE

$$w' + \mathbf{v}.\nabla w = 0. \tag{2.23}$$

Suppose $\mathbf{v}$ is constant. There now exists a closed form solution. Let us consider the one dimensional counterpart of the above equation, namely

$$\frac{\partial w}{\partial t} + v\frac{\partial w}{\partial x} = 0. \tag{2.24}$$

Suppose mass w at a location x and time t is given by an arbitrary function f,

$$w(x, t) = f(x - vt) \tag{2.25}$$

where v is a constant. Then differentiating with respect to t and x, we get

$$\frac{\partial w}{\partial t} = -vf'(x - vt) \tag{2.26}$$
$$\frac{\partial w}{\partial x} = f'(x - vt). \tag{2.27}$$

The above expressions satisfies equation (2.24) and (2.25) is considered as a general solution of equation (2.24). To see this, we shall introduce the characteristic coordinates

$$\xi = x - vt, \tag{2.28}$$
$$\eta = x + vt \tag{2.29}$$

so that

$$x = \frac{1}{2}(\xi + \eta), \tag{2.30}$$
$$t = \frac{\eta - \xi}{2v}. \tag{2.31}$$

Also we write $w(x, t) = \tilde{w}(\eta, \xi)$. Then

$$\frac{\partial w}{\partial t} = \frac{\partial \tilde{w}}{\partial \eta}\frac{\partial \eta}{\partial t} + \frac{\partial \tilde{w}}{\partial \xi}\frac{\partial \xi}{\partial t} = v\frac{\partial \tilde{w}}{\partial \eta} - v\frac{\partial \tilde{w}}{\partial \xi}, \tag{2.32}$$
$$\frac{\partial w}{\partial x} = \frac{\partial \tilde{w}}{\partial \eta}\frac{\partial \eta}{\partial x} + \frac{\partial \tilde{w}}{\partial \xi}\frac{\partial \xi}{\partial x} = \frac{\partial \tilde{w}}{\partial \eta} + \frac{\partial \tilde{w}}{\partial \xi}. \tag{2.33}$$

Since w is assumed to be the solution, we have

$$\frac{\partial w}{\partial t} + v\frac{\partial w}{\partial x} = 0. \tag{2.34}$$

Now using (2.32) and (2.33) in (2.34), we get

$$v\frac{\partial \tilde{w}}{\partial \eta} - v\frac{\partial \tilde{w}}{\partial \xi} + v\frac{\partial \tilde{w}}{\partial \eta} + v\frac{\partial \tilde{w}}{\partial \xi} = 0. \tag{2.35}$$

This implies that

$$\frac{\partial \tilde{w}}{\partial \eta} = 0, \tag{2.36}$$

hence $\tilde{w}$ is independent of variable η. Thus $\tilde{w}$ is a function of ξ only and we can write

$$\tilde{w} = \tilde{w}(\xi) \tag{2.37}$$

$$= \tilde{w}(x - vt). \tag{2.38}$$

Also for $t = 0$, it follows that

$$w(x, 0) = f(x). \tag{2.39}$$

This is called a wave profile. As time progresses, this wave profile moves to the right. When velocity of the wave is negative, the equation takes the form

$$\frac{\partial w}{\partial t} - v\frac{\partial w}{\partial x} = 0, \tag{2.40}$$

whose general solution is given by

$$w(x, t) = f(x + vt). \tag{2.41}$$

As time t increases wave profile moves to left. Thus the one dimensional hyperbolic equation has solutions which are necessarily travelling waves. This property is also shared by higher dimensional first order PDEs. Thus when $\mathbf{v}$ is constant, the solutions of hyperbolic PDE

$$w' + \mathbf{v}.\nabla w = 0 \tag{2.42}$$

are travelling waves in higher dimensions. When $\mathbf{v}$ is nonconstant but a function $\mathbf{v} = \mathbf{v}(x)$, a similar method of solutions again leads to travelling solutions. However, the assumption $\mathbf{v} = \mathbf{v}(x)$ can lead to what are known as shocks. This means a dramatic change in the mass of species over a small time period, **i.e**. a singularity in the gradient of mass w.

The seemingly simple system of partial differential equations (2.21), (2.22) is in fact quite complicated to analyze. Very little known about its mathematical properties, if its inherited from parabolic - like first equation (2.21) or hyperbolic - like second equation or if its behavior entirely different from either type. We would like to investigate if the system develops shocks or are its solutions smooth function of x for all time t. Indeed, its equlibria correspond to the solutions of the system

$$n' = 0 \tag{2.43}$$

$$w' = 0. \tag{2.44}$$

This gives a coupled system of PDEs in the spatial variable x,

$$\mu\Delta n = B - D \tag{2.45}$$

$$\mu(\frac{\nabla n.\nabla w}{n}) = G. \tag{2.46}$$

Such systems can have multiple solutions. Among the possible solutions are the spatially homogeneous ones,

$$B(n, w) = D(n, w) \tag{2.47}$$

$$G(n, w) = 0. \tag{2.48}$$

These are indeed the equlibria for system of ODEs. Also it is not known if these are the only solutions of the spatially dependent equlibrium equations (2.45) and (2.46). Nevertheless, in spite of lack of well developed theory for the system (2.21), (2.22), it still offers an attractive approach to modeling mass and space dependent population dynamics.

2.3 Derivation of Growth Model

To derive the growth model, we first assume spatially uniform distributions, that is, $n(t)$ and $w(t)$ are functions of time only where $n(t)$ denotes the number of individuals and $w(t)$ denotes the mass per individual. Let $\rho(t) := n(t)w(t)$ denote the biomass density. We now discuss the mathematical representations of nonlinear birth $B(n, w)$, death $D(n, w)$ and growth $G(n, w)$ processes,

$$B(n, w) = \beta \left(\frac{w}{w_m}\right) n \left(1 - \frac{\rho}{K}\right) \tag{2.49}$$

$$D(n, w) = d\, n \tag{2.50}$$

$$G(n, w) = \psi \, (w_m - w) \left(1 - \frac{\rho}{K}\right) \tag{2.51}$$

where β, d and ψ are instantaneous birth, death and growth rates that can be functions of mass w. Here w_m is the characteristic mass defined as the "maximum mass" an individual can attain. Before the carrying capacity K is defined, it is important to know the meaning of the term "parent stock". In fisheries "parent stock" means spawning stock biomass and according to the definition of ICES [22] this means total weight of all sexually mature fish in the stock. The carrying capacity in the parent stock K is the total biomass per unit domain. Nonlinear birth function (2.49) says how the number of individuals in a population changes due to instantaneous birth rate β which is modified by density dependence and mass. Density dependent death is given by (2.50). The mathematical representation for nonlinear growth function (2.51) shows how mass changes due to instantaneous growth rate ψ. Also it is important to note that this is von Bertalanffy type of growth equation [75], the rate of growth of an individual declines with its maximum mass (that is, mass is capped by the maximum mass the environment can support).

2.3.1 Conservation Laws for Spatially Uniform Distribution

The model to track number of individuals takes the form

$$n'(t) = B(n(t), w(t)) - D(n(t), w(t)). \tag{2.52}$$

Equation (2.52) says how number of individuals changes due to birth and death at time t. The growth equation for mass $w(t)$ is derived considering how the biomass $\rho(t)$ evolves due to birth, death and growth. To that end, we consider the biomass balance

$$\rho'(t) = n(t)G(n(t), w(t)) + w_b\, B(n(t), w(t)) - D(n(t), w(t))\, w, \tag{2.53}$$

where w_b denote the birth mass. Differentiating biomass density $\rho(t)$

$$\rho(t) = n(t)\, w(t) \tag{2.54}$$

with respect to time t, one gets

$$\rho'(t) = n'(t)w(t) + n(t)w'(t). \tag{2.55}$$

Rewriting the above expression for change in the mass $w'(t)$, we have

$$w'(t) = \frac{\rho'(t)}{n(t)} - \frac{n'(t)w(t)}{n(t)}. \tag{2.56}$$

Now using expression for change in number of individuals (2.52) and change in biomass (2.53) in (2.56) and after doing some algebra, we get the growth model

$$w'(t) = G(n(t), w(t)) + \frac{B(n(t), w(t))}{n}(w_b - w). \tag{2.57}$$

One can augment (2.52) and (2.57) with spatial transport terms to obtain the system of partial differential equations to track density and mass of a population at a space variable x and time t

$$n' - \mu \Delta n = B(n, w) - D(n, w) \tag{2.58}$$

$$w' - \mu \left(\frac{\nabla n . \nabla w}{n} \right) = \frac{B(n, w)}{n}(w_b - w) + G(n, w). \tag{2.59}$$

The coupled nonlinear system of PDEs (2.58) and (2.59) arising from our modeling effort will be henceforth referred to as the density and mass model. As a first step to understanding our model, we reduce the model to 1-D system of coupled nonlinear parabolic-hyperbolic partial differential equations

$$\frac{\partial n}{\partial t} = \mu \left(\frac{\partial^2 n}{\partial x^2} \right) + B(n,w) - D(n,w) \tag{2.60}$$

$$\frac{\partial w}{\partial t} = \mu \, \frac{1}{n} \left(\frac{\partial n}{\partial x} \right) \left(\frac{\partial w}{\partial x} \right) + \frac{B(n,w)}{n}(w_b - w) + G(n,w), \tag{2.61}$$

where $n(x,t)$, $w(x,t)$ are the density, mass of a population respectively. Here $B(n,w)$, $D(n,w)$ and $G(n,w)$ are the nonlinear birth, death and growth terms defined above (2.49) - (2.51). Also μ is the transport coefficient, and w_b is the mass at birth.

Equation (2.60) gives density of the population at a location x and time t. It is controlled by three processes: transport, reproduction and mortality. The first term describes diffusion: random motion of a population. The second term represents density dependent reproduction and the last term denotes the density dependent death. The mass of a population at a location x and time t is given by (2.61) and is controlled by three processes: transport, reproduction and growth . The first term describes transport of a population. The second term represents change in mass due to birth mass and reproduction (negative sign signifies as birth increases the mass goes down i.e individuals are born with a smaller size). The third term captures change in the mass due to growth and also shows mass is capped.

The PDE system is difficult to analyze, but the ODE system is tractable. In the next chapter, we briefly discuss a theoretical analysis of the spatially constant equilibria.

3. DENSITY AND MASS MODEL WITH MASS DEPENDENT TRANSPORT COEFFICIENTS

3.1 Governing System of Partial Differential Equations

The assumption that the transport coefficient depends on the mass applied to the system of coupled nonlinear parabolic (2.60) and hyperbolic (2.61) PDE discussed in Section 2.3 yields a system of coupled nonlinear reaction diffusion-hyperbolic PDEs to track density and mass of a population at location x and time t. For illustrative purposes, we consider a mass dependent transport coefficient $\mu = \mu_1(w)$ of the form:

$$\mu = \mu_1 \left(1 - \frac{w}{w_m}\right) \tag{3.1}$$

giving rise to the system of partial differential equations

$$\frac{\partial n}{\partial t} = \mu_1 \left(1 - \frac{w}{w_m}\right)\left(\frac{\partial^2 n}{\partial x^2}\right) - \mu_1 \frac{\partial n}{\partial x}\frac{\partial w}{\partial x} + B(n,w) - D(n,w) \tag{3.2}$$

$$\frac{\partial w}{\partial t} = \mu_1 \left(1 - \frac{w}{w_m}\right)\frac{1}{n}\left(\frac{\partial n}{\partial x}\right)\left(\frac{\partial w}{\partial x}\right) + \frac{B(n,w)}{n}(w_b - w) + G(n,w) \tag{3.3}$$

where $n(x,t)$, $w(x,t)$ are the density and mass of a population, respectively at a spatial variable x and time t, all other quantities are as previously defined. The constitutive choice (3.1) means when mass approaches the maximum mass, that is, when the species grows to its maximum size, diffusive transport gets shuts down, that is, the system is driven to equilibrium. Now substituting the nonlinear functions $B(n,w)$, $D(n,w)$ and $G(n,w)$ from Section 2.3 in above reaction-diffusion and hyperbolic system of partial differential equations (3.2) and (3.3),

$$\frac{\partial n}{\partial t} = \mu_1 \left(1 - \frac{w}{w_m}\right) \left(\frac{\partial^2 n}{\partial x^2}\right) - \mu_1 \, \frac{\partial n}{\partial x} \, \frac{\partial w}{\partial x} + \beta \, \left(\frac{w}{w_m}\right) n \left(1 - \frac{\rho}{K}\right) - d \, n \tag{3.4}$$

$$\frac{\partial w}{\partial t} = \mu_1 \left(1 - \frac{w}{w_m}\right) \frac{1}{n} \left(\frac{\partial n}{\partial x}\right) \, \left(\frac{\partial w}{\partial x}\right) + \beta \, \left(\frac{w}{w_m}\right) \left(1 - \frac{\rho}{K}\right) (w_b - w)$$
$$+ \psi \, (w_m - w) \left(1 - \frac{\rho}{K}\right). \tag{3.5}$$

Our assumption is that the system under consideration is closed in the sense that individuals in a population are being isolated from the outside world. The mathematical condition arising from this biological property is that there is no flux of any individuals through the boundary [84]. Thus, for a closed ecosystem, the system of PDEs must be augmented by initial conditions,

$$n(x, 0) = n_0(x), \;\; w(x, 0) = w_0(x), \tag{3.6}$$

and no-flux boundary conditions,

$$n_x(t, a) = 0, \;\; n_x(t, b) = 0 \tag{3.7}$$

$$w_x(t, a) = 0, \;\; w_x(t, b) = 0, \tag{3.8}$$

where $[a, b]$ is the domain length. Equation (3.4) helps to track density of the population at location 'x' and time 't'. It is controlled by four processes: diffusion, transport, reproduction and mortality. The first term in the right hand side of equation (3.4) describes diffusion, that is, random motion of species with a mass dependent coefficient. The second term of equation (3.4) shows how transport brings in change in density. Density dependent reproduction and death are represented by the third and the fourth term of equation (3.4) respectively.

The mass of species at location x and time t is given by (3.5) and is controlled by three processes: transport, reproduction and growth. The first term in the right hand side of equation (3.5) describes transport of species with mass dependent coefficient. The second term of equation (3.5) represents change in mass due to reproduction (negative sign signifies as birth increases the average mass goes down). The third term of equation (3.5) captures change in the average mass due to growth, and it shows average mass is capped by the mass which the environment can support.

We now discuss the dimensions of the variables and the parameters in the above system. Number density $n(x,t)$ is the total number of individuals per unit domain length with dimensions $\frac{N}{L}$. In one-dimension the domain is a unit line, and in two-dimensions, the domain is a unit area. Average mass $w(x,t)$ is mass per individual with dimensions $\frac{KG}{N}$. The carrying capacity in the parent stock 'K' is the total biomass per unit domain length with dimensions $\frac{KG}{L}$.

Parameters ψ, β and d are maximum instantaneous individual per capita average growth rate with dimensions $\frac{1}{T}$, maximum instantaneous per capita birth rate with dimensions $\frac{1}{T}$ and natural instantaneous per capita mortality rate with dimensions $\frac{1}{T}$. The transport coefficient is given by μ with dimensions $\frac{L^2}{T}$. In order to reduce the number of parameters, we shall non-dimensionalize the system of reaction-diffusion (3.4) and hyperbolic (3.5) equations. To rescale time t, one can choose

$$t = \frac{\tilde{t}}{\beta}, \quad t = \frac{\tilde{t}}{d}, \quad t = \frac{\tilde{t}}{\psi}. \tag{3.9}$$

Our choice is

$$t = \frac{\tilde{t}}{\beta}. \tag{3.10}$$

We define L_m, a constant used to rescale the spatial variable x. We introduce the following non-dimensionalization

$$\tilde{n} = \frac{n}{K_m}, \quad \tilde{w} = \frac{w}{w_m} \quad \tilde{t} = \beta t, \quad \tilde{x} = \frac{x}{L_m} \tag{3.11}$$

where w_m is the characteristic mass defined as the "maximum mass individual can attain" and K_m is the characteristic density, say

$$K_m = \frac{K}{w_m}. \tag{3.12}$$

Using dimensionless variables, (3.11) and (3.12) in system of partial differential equations (3.4) and (3.5), and dropping the tildes on the dimensionless variables,

$$\frac{\partial n}{\partial t} = a\,(1-w)\frac{\partial^2 n}{\partial x^2} - a\frac{\partial n}{\partial x}\,\frac{\partial w}{\partial x} + n\,w(1-nw) - bn \tag{3.13}$$

$$\frac{\partial w}{\partial t} = a(1-w)\frac{1}{n}\left(\frac{\partial n}{\partial x}\right)\,\left(\frac{\partial w}{\partial x}\right) + w(1-nw)\,(W_b - w) + c\,(1-nw)(1-w) \tag{3.14}$$

where n is density, w is mass of the population, W_b is the non-dimensional birth mass

$$W_b = \frac{w_b}{w_m}. \tag{3.15}$$

The dimensionless ratios of transport, death, growth rates are given by

$$a = \frac{\mu}{\beta\,{L_m}^2},\; b = \frac{d}{\beta},\; c = \frac{\psi}{\beta}, \tag{3.16}$$

respectively.

In the following Section, we present a very brief theoretical analysis of the governing system of differential equations, (3.13) and (3.14). The PDE system is difficult to analyze, but the ODE counterpart is tractable. We now include an analysis of the spatially constant equilibria.

3.2 Theoretical Analysis of the Spatially Uniform Density and Mass Model

The spatially uniform density and mass model discussed in Chapter 2, Section 2.3 will be considered here. The system of ordinary differential equations to track density and mass of a population are given by equations (2.52) and (2.57), respectively

$$n'(t) = B(n(t), w(t)) - D(n(t), w(t)), \tag{3.17}$$

$$w'(t) = G(n(t), w(t)) + \frac{B(n(t), w(t))}{n}(w_b - w). \tag{3.18}$$

The corrresponding dimensionless system of ordinary differential equations is

$$\frac{dn}{dt} = n\, w(1 - nw) - bn \tag{3.19}$$

$$\frac{dw}{dt} = c\,(1 - nw)\,(1 - w) + w(1 - nw)\,(W_b - w)\,. \tag{3.20}$$

Here n is the density, w is the mass per individual (average mass). Here dimensionless ratio b takes two forms. In the non-fishing domain, b will be defined as b_n,

$$b_n = \frac{d}{\beta}. \tag{3.21}$$

where d is the natural instantaneous per capita mortality rate, and β is the maximum instantaneous per capita birth rate. On the fishing domain, b is defined as b_f, where

$$b_f = \frac{d + f}{\beta} \tag{3.22}$$

where f is the instantaneous fishing mortality rate. Also

$$c = \frac{\psi}{\beta}, \;\; W_b = \frac{w_b}{w_m}. \tag{3.23}$$

To find all the equilibria of system of ODEs (3.19) and (3.20), we set the right hand side of the above system to zero.

$$nw(1 - nw) - bn = 0 \tag{3.24}$$

$$c\,(1 - nw)\,(1 - w) + w(1 - nw)\,(W_b - w) = 0 \tag{3.25}$$

After doing a little bit of algebra, we have two sets of equilibrium points (n^*, w^*).

$$(n^*, w^*) = (0, 0) \tag{3.26}$$

$$(n^*, w^*) = \left(\frac{1 - \frac{b}{w^*}}{w^*}, \frac{-(c - W_b) \pm \sqrt{(c - W_b^2) + 4c}}{2} \right) \tag{3.27}$$

3.2.1 Condition for Positive Equilibria, Yield, and an Expression for Maximum Sustainable Fishing Rate

In the present Subsection, some important conditions to obtain the positive equilibria for the system of ODEs (3.19) and (3.20) will be discussed. To that end, we get an expression for maximum sustainable fishing rate. In order to analyse the spatial equilibrium points, we have the following theorem,

Theorem 3.2.1. *(1) The system of ordinary differential equations (3.19) and (3.20) has a positive equilibrium if the following condition hold,*

$$\frac{b}{w^*} \leq 1, \tag{3.28}$$

where w^* *is the equilibrium average mass and* b *is the non dimensional ratio. Biologically this means, mass should always be greater than the non dimensional ratio* b *for the system to have positive equlibria. One can substitute,*

$$b = \frac{d+f}{\beta} \tag{3.29}$$

in the above condition (3.28) and get an expression

$$\beta w^* - d \geq f. \tag{3.30}$$

The upper bound of fishing rate f *in the expression (3.30), for which one obtains a positive stable equilibrium, will be defined as the maximum fishing rate, denoted as* f_{max}*, that is,*

$$\beta w^* - d = f_{max}. \tag{3.31}$$

(2) Indeed, the above expression (3.31) turns out to be the condition for biomass yield at equilibrium to be positive, that is,

$$Y = f \;\; n^* \;\; w^* > 0. \tag{3.32}$$

Here yield is the catch in weight. It is measured in tons. In fisheries, catch and yield are often used interchangeably. Substituting the equilibrium point for density n^**, in the expression (3.32), we get*

$$Y = f \;\; \left(\frac{1 - \frac{b}{w^*}}{w^*}\right) w^*. \tag{3.33}$$

Using the dimensionless ratio b *from equation (3.29) in the expression for biomass* *yield (3.33) and simplifying we get*

$$Y = \frac{f}{\beta w^*} \ \big((\beta w^* - d) - f \big). \tag{3.34}$$

From equation (3.34), it is clear that the condition for biomass yield to be positive, is

$$\beta w^* - d \geq f. \tag{3.35}$$

Equation (3.35) is same as (3.30).

Our aim is to find an expression for maximum sustainable fishing rate f_S for which we get maximum sustainable biomass yield (MSBY), in turn, this allows to harvest a marine population sustainably. The sustainable fishing rate means the fishing rate at which number (weight) of fish in a stock that can be taken out by fishing without reducing the stock biomass, assuming that environmental conditions remain the same [63].

MSBY is the maximum catch in weight that can be caught without depleting the population. So, we consider the expression (3.22) for dimensionless ratio b. Before deriving an expression for maximum sustainable fishing rate f_S, we list the possible definitions of fishing rates which will be used in this dissertation.

1) f is the instantaneous fishing mortality rate.

2) f_{max} is the maximum fishing rate that gives a positive stable equilibrium.

3) f_S is the fishing rate that gives MSY in biomass, under a ODE model.

4) $f_S^{'}$ is the fishing rate within a fishing zone which gives MSBY, (over the entire space) in a PDE model.

MSBY occurs when

$$\frac{dY}{df} = 0, \tag{3.36}$$

that is,

$$\frac{dY}{df} = 1 - \frac{d}{\beta w^*} - \frac{2f}{\beta w^*} = 0. \tag{3.37}$$

Solving the equation (3.37) for f,

$$f = \frac{\beta w^* - d}{2}. \tag{3.38}$$

Therefore, MSBY occurs when condition (3.38) holds. When fishing rate f satisfies condition (3.38), we have sustainability. Using expressions (3.31) and (3.37), we define maximum sustainable fishing rate f_S,

$$f_S \ = \ \frac{\beta w^* - d}{2} = \frac{f_{max}}{2} \ < f_{max}. \tag{3.39}$$

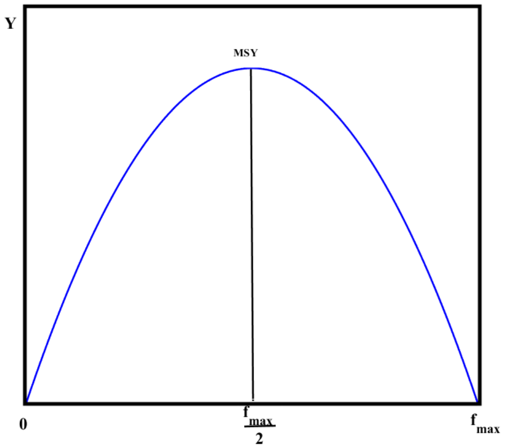

Figure 3.1: Maximum sustainable biomass yield at maximum sustainable fishing rate

4. FINITE DIFFERENCE METHOD FOR A SYSTEM OF COUPLED NONLINEAR REACTION-DIFFUSION AND HYPERBOLIC PDES

Finite difference method (FDM) is one of the simplest and oldest approximation approaches to solve the ODEs and PDEs. In this method we use the calculus of finite differences to develop an approximation formula. The theoretical foundation for this method is based on the Taylor's series expansion.

This method was used by L. Euler in 1768 to solve differential equations in one dimension of space and extended to two dimensions by C. Runge in 1908. In 1928, FDM was further established in a fundamental theoretical paper by Courant, Friedrichs, Lewy [16]. Around 1950's, with the emergence of computer the FDM was used to solve time-dependent problems. Since then, FDM has been extensively used to study significant problems in scientific and engineering fields.

Shortly after British Researchers Crank and Nicolson briefly described methods of evaluating numerical solutions of PDE [17], John Von Neumann came up with a more meticulous treatment in an article [14]. He established Von Neumann stability analysis (also known as Fourier stability analysis) which is used to check the stability of finite difference schemes when applied to linear PDEs. Therefore these two decades (1950s and 1960s) were the intense period of development of the finite difference theory for general initial value problems and parabolic problems. Around the same time, the concept of stability was explored in the *Lax equivalence theorem* [43] and the *Kreiss matrix lemmas* [77]. Further major contributions regarding stability and apriori estimates are given by Douglas, Lees, Samarskii, Widlund and others [81]. Starting with work by Friedrichs [19], Lax [44], and Wendroff [85] for hyperbolic equations, and particularly for nonlinear conservation laws, the FDM has continually played a major role up until now. Error analysis for the elliptic partial differential equations was first worked by Gerschgorin [20]. In the 1950's and 1960's a large number of works on systems associated with finite difference approximation of second-order elliptic equations, for example, the five-point scheme were developed [67], [74]. Over the past six decades, theories have been established with regard to accuracy, stability and convergence of finite difference scheme for differential equations.

Partial differential equations act as a bridge between applied mathematics and pure mathematics [7]. Empirically, most PDEs are studied computationally. There are two ways to approach this. The first approach is based on the classical numerical analysis. In this method, error estimates of an approximation problem are obtained on a finite dimensional space, with more rigorous arguments. The second approach is based purely on computations, in which one might compute the solution of a simplified model without worrying much about the mathematical analysis. There is always an uncertainity and controversies about the validity of the computational results particularly when the result is difficult to analyze theoretically, for example, estimating the optimal harvesting rate that helps to harvest a population sustainably.

In summary, the history reveals the fact that there has been a vast development of mathematical methods to analyze and solve the PDEs arising in different areas of science. Computational methodologies acts as an important experimental tool to spark off conjectures for analytic arguments, and the study of numerical simulations serves as a source of suggestions for rigorous treatment of PDEs [7]. Thus, the triad of methodologies, theoretical, experimental and computational, helps us to solve some of the most difficult and fundamental problems in mathematics.

4.1 Implemention of Finite Difference Method

In order to implement FDM, one must generate a mesh with grid points (x_i, t_j), where we want to find an approximate solutions. Then, we replace the derivative terms in a partial differential equation by divided difference formulae at each grid point, producing a system of algebraic equations. The numerical solution of these algebraic equations are discrete equations; this is the characteristic part of numerical analysis of partial differential equations. Finally, the error analysis can be done by analysing stability, consistency, convergence for the given partial differential equation and error analysis in the numerical results is done by using grid convergence technique.

4.2 Finite Difference Approximations

Suppose we want to approximate $f'(x)$. Using the definition of derivative we have

$$f'(x) = \lim_{h \to 0} \frac{f(x+h) - f(x)}{h}. \tag{4.1}$$

We discretize the domain of a given function $f(x)$ with a set of points $x_i, \quad i = 0, 1, 2, N$ and define the sequence of x_i values in terms of mesh size h, that is,

$$x_{i+1} = x_i + h. \tag{4.2}$$

Then the definition (4.1) at a discrete point x_i can be written as

$$\begin{aligned} f'(x_i) &= \lim_{h \to 0} \frac{f(x_i + h) - f(x_i)}{h} \\ &= \frac{f_{i+1} - f_i}{h} \end{aligned} \tag{4.3}$$

where h is sufficiently small. This formula uses the forward difference approximation and hence the name forward Euler approximation [69]. Similarly there are two other difference approximations. Backward Euler and Central difference approximations [69] are given by

$$\begin{aligned} f'(x_i) &= \lim_{h \to 0} \frac{f(x_i) - f(x_i - h)}{h} \\ &= \frac{f_i - f_{i-1}}{h}, \end{aligned} \tag{4.4}$$

$$\begin{aligned} f'(x_i) &= \lim_{h \to 0} \frac{f(x_i + h) - f(x_i - h)}{h} \\ &= \frac{f_{i+1} - f_{i-1}}{2h} \end{aligned} \tag{4.5}$$

respectively. Now the obvious question is "which is a better approximation?" To answer this question and also to analyze the error in the difference approximation, one might have to use a Taylor's series. The Taylor series expansion of function f about the point x_i is given by

$$f(x_i + h) = f(x_i) + hf'(x_i) + \frac{1}{2}h^2 f''(x_i) + \frac{1}{6}h^3 f'''(x_i) + O(h^4). \tag{4.6}$$

Here $O(\cdot)$ is the big O notation. It is important to note that Taylor's series expansions are valid when f is sufficiently smooth. Now rearranging the terms in the above series, we get

$$\frac{f(x_i + h) - f(x_i)}{h} - f'(x_i) = \frac{1}{2}hf''(x_i) + \frac{1}{6}h^2 f'''(x_i) + O(h^3). \tag{4.7}$$

The error in forward Euler approximation is given by this expression (4.7). The expression in the right hand side of the above expression can be referred to as truncation error, which is the error obtained by truncating the series. Similarly, we can derive truncation errors for backward Euler and central difference approximations. Expanding the function values of f about the point x_i, we get

$$f(x_i - h) = f(x_i) - hf'(x_i) + \frac{1}{2}h^2 f''(x_i) - \frac{1}{6}h^3 f'''(x_i) + O(h^4) \tag{4.8}$$

which on rearranging gives the truncation error for backward Euler,

$$\frac{f(x_i) - f(x_i - h)}{h} - f'(x_i) = -\frac{1}{2}hf''(x_i) + \frac{1}{6}h^2 f'''(x_i) + O(h^3). \tag{4.9}$$

The truncation error for forward and backward Euler approximations are proportional to h and hence these approximations are referred to as first order approximations. Now combining equations (4.6) and (4.8) , we get

$$f(x_i + h) - f(x_i - h) = 2hf' + \frac{1}{3}h^3 f'''(x_i) + O(h^5). \tag{4.10}$$

This can be further reduced in the form,

$$\frac{f(x_i + h) - f(x_i - h)}{h} - f'(x_i) = \frac{1}{6}h^2 f'''(x_i) + O(h^4) \tag{4.11}$$

This shows that the truncation error is proportional to h^2 and hence the approximation is referred to as second order approximation. Now we illustrate finite difference approximation using two examples.

Example 1: We now briefly discuss finite difference formulation for second order non-homogeneous Dirichlet problem. Suppose $u : \bar{\Omega} \to \mathbb{R}$ for a bounded domain $\Omega = (0, 1) \subset \mathbb{R}$. Here $\bar{\Omega} = \Omega \cup \partial\Omega$, where $\partial\Omega$ is the boundary.

$$-u'' + c\, u(x) = f(x) \tag{4.12}$$

$$u(0) = \alpha, u(1) = \beta \tag{4.13}$$

Equations (4.12) and (4.13) together represent 1D-BVP, where $c \in \mathbb{R}$, $f(x)$ is any given function of x, defined on $\bar{\Omega}$, $c \geq 0$. Here

$$x_i = ih, \;\; 0 \leq i \leq N+1, \tag{4.14}$$

is the grid point and

$$h = \frac{1}{N+1} \tag{4.15}$$

is the mesh width (distance between any two grid points x_i and x_{i+1}), N is an integer. At each of these grid points, we attempt to compute a numerical value of the solution

$$U_0, \; U_1, \; U_2, \; ..., U_N, \; U_{N+1} \tag{4.16}$$

where U_i is the approximation to the solution $u(x_i)$. Now using the boundary conditions from equation (4.13),

$$U_0 = \alpha, \;\; U_{N+1} = \beta. \tag{4.17}$$

We now have N unknowns to compute: $U_1, U_2, ..., U_N$. By replacing the second order derivative by central difference approximation, we obtain

$$\frac{U_{i+1} - 2U_i + U_{i-1}}{h^2} + c\, U_i = F_i \tag{4.18}$$

where $U_i = u(x_i)$ and $F_i = f(x_i)$. The example discussed above gives an essence of the finite difference scheme. The reader is directed to references [69, 78] for different types of finite difference schemes for both ODEs and PDEs.

Example 2: In this illustration, we consider a one dimensional parabolic PDE, which is a time dependent problem. We want to find $u : [0,T] \times \bar{\Omega} \to \mathbb{R}$ such that

$$\frac{\partial u}{\partial t} - \frac{\partial^2 u}{\partial x^2} + c\, u(x,t) = f(x,t),\ x \in (0,1),\ t \geq 0 \tag{4.19}$$

$$u(0,t) = u(1,t) = 0, \qquad t \geq 0 \tag{4.20}$$

$$u(x,0) = u_0(x),\ x \in (0,1) \tag{4.21}$$

Under limiting conditions, one obtains two point BVP (4.12). We formulate a grid with grid points (x_i, t_n) , where

$$x_i = ih, \quad t_n = nk. \tag{4.22}$$

Here $h = \Delta x$ is the mesh spacing on the spatial axis x and $k = \Delta t$ is the time step. Suppose U_i^n is the numerical approximation to the solution $u(x_i, t_n)$ at the grid point (x_i, t_n),

$$U_i^n \approx u(x_i, t_n). \tag{4.23}$$

Then using forward difference approximation for time derivative and central difference approximation for space derivative, we get

$$\frac{U_i^{n+1} - U_i^n}{k} = \frac{U_{i+1}^n - 2U_i^n + U_{i-1}^n}{h^2} + c\, U_i^n + F_i^n, \tag{4.24}$$

where $F_i^n = f(x_i, t_n)$. We refer to the above forward time central space approximation as the finite difference scheme for given PDEs (4.19). Now rearranging scheme (4.24),

$$U_i^{n+1} = U_i^n + \frac{k}{h^2}\left(U_{i+1}^n - 2U_i^n + U_{i-1}^n\right) + c\, k\, U_i^n + kF_i^n. \tag{4.25}$$

Using the above equation (4.25), one can compute U_i^{n+1} explicitly using the values from the previous time step and hence the name an explicit method. For the sake of simplicity, we set $c = 0$ and $f = 0$ in equation (4.19). Then the PDE (4.19) reduces to

$$\frac{\partial u}{\partial t} = \frac{\partial^2 u}{\partial x^2} \tag{4.26}$$

The corresponding scheme for (4.26) is

$$U_i^{n+1} = U_i^n + \frac{k}{h^2}\left(U_{i+1}^n - 2U_i^n + U_{i-1}^n\right). \tag{4.27}$$

We now briefly discuss the local truncation error of explicit method (4.27). To that end, we discuss the convergence analysis of finite difference scheme for a linear partial differential equation. Local truncation error is the discrepancy one obtains when the discretized solution is replaced by the true solution in the finite difference formula. Then the local truncation error is given by

$$\tau_i^n = \tau(x_i, t_n), \tag{4.28}$$

where

$$\tau(x,t) = \frac{u(x,t+k) - u(x,t)}{k} - \frac{1}{h^2}(u(x-h,t) - 2u(x,t) + u(x+h,t)). \tag{4.29}$$

For a smooth function $u(x,t)$, using Taylor's series expansion of u with respect to t (keeping x fixed),

$$u(x,t+k) = u(x,k) + ku_t + \frac{1}{2}k^2 u_{tt} + ... + O(k^n). \tag{4.30}$$

Rearranging, we get

$$\frac{u(x,t+k)-u(x,t)}{k} = u_t + \frac{1}{2}ku_{tt} + \frac{1}{6}k^2u_{ttt} + ... \tag{4.31}$$

Similarly one can expand $u(x-h)$ and $u(x+h)$ (using Taylor's series) with respect to x (fixing t),

$$(u(x-h,t) - 2u(x,t) + u(x+h,t)) = h^2\big(u_{xx} + \frac{1}{2}h^4u_{xxxx} + ...\big). \tag{4.32}$$

Then using equations (4.30) and (4.32) in (4.29),

$$\tau(x,t) = \big(u_t + \frac{1}{2}ku_{tt} + \frac{1}{6}k^2u_{ttt} + ...\big) - \big(u_{xx} + \frac{1}{2}h^2u_{xxxx} + ...\big) \tag{4.33}$$

Now using equation (4.26)

$$u_t = u_{xx} \tag{4.34}$$

and the derivative of (4.26) with respect to t,

$$u_{tt} = u_{txx} = u_{xxxx} \tag{4.35}$$

in (4.33) we have the local truncation error

$$\tau(x,t) = \left(\frac{1}{2}k - \frac{1}{12}h^2\right)u_{xxxx} + O(k^2 + h^4). \tag{4.36}$$

This method is second order accurate in space and first order accurate in time, since $O(h^2 + k)$. There are several important results and estimates for equation (4.19) with applications in the field of biology [36].

So from the two illustrations, one can infer that the finite difference scheme results from an approximation of a given equation using a Taylor expansion. The discussion of local truncation error leads to the concept of consistency. The notion of consistency helps one to understand how well a finite difference scheme approximates an equation. A finite difference method is said to be consistent if $\tau(x,t) \to 0$ as $k, h \to 0$. To analyze stability of the numerical scheme, one must define a norm on $\mathbb{R}^N$:

$$\|u\|_p = \big(\sum_{j=1}^{N} |u_j|^p\big)^{\frac{1}{p}}. \tag{4.37}$$

Note: $p = 1$ is L^1 norm, $p = 2$ is L^2 norm, and $p = \infty$ is L^∞ norm.

We now discuss the consistency, stability and convergence for general class of linear partial differential equations [78],

$$F(\partial_x, \partial_t)u = g(x,t). \tag{4.38}$$

For the uniqueness of solution for (4.38), one needs to specify the initial conditions. Thus the initial conditions are of the form,

$$u(x,0) = u_0(x). \tag{4.39}$$

Definition 1. Given a partial differential equation (4.38) and the corresponding finite difference scheme, $F_{h,k}U = g$, we say that the scheme is consistent with the PDE if for any smooth function $\phi(x,t)$

$$F\phi - F_{h,k}\phi \to 0 \ \ as \ \ h, k \to 0. \tag{4.40}$$

Here, F is the continuous operator (with partial derivatives) and $F_{h,k}$ is the discrete operator (with finite differences). We now discuss the concept of stability for a homogeneous initial value problem, i.e. $g = 0$ in (4.38). We define the stability region as any bounded nonempty region of the first quadrant of R^2.

Definition 2. A finite difference scheme $F_{h,k}U_i^n = 0$ for a first order equation is stable in a stability region if there is an integer J such that for $T > 0$, there is a constant C_T such that

$$\|U^n\|_p \leq C_T \sum_{j=0}^{N} \left\|U^j\right\|_p . \tag{4.41}$$

for all n with $0 \leq nk \leq T$, p represents the norm (L^1, L^2, L^∞- norm).

Interpretation: The above norm inequality express the idea that the norm of the solution at any time t, is limited in the amount of the growth that can occur. Hence stability.

Definition 3. A one-step finite difference scheme approximating a partial differential equation (4.38) is a convergent scheme if for any solution to the partial differential equation, $u(x,t)$, and solutions to the finite difference scheme, ${U_i}^n$, such that ${U_i}^0$ converges to $u_0(x)$ as ih converges to x, then ${U_i}^n$ converges to $u(x,t)$ as (ih, nk) converges to (x,t) as h, k converge to zero. It is also important to note that the concept of stability is closely related to concept of well-posedness for initial value problems (IVPs) for PDEs.

Definition 4. The initial value problem for a first order partial differential equation $Fu = 0$ is well posed if for each positive T there is a constant C_T such that

$$\|U^n\|_p \leq C_T \left\|U^0\right\|_p . \tag{4.42}$$

hold for all initial data. Here the constant C_T is independent of the solution.

The significance of the four definitions discussed above is seen in the Lax-Richtmeyer equivalence theorem, which is the fundamental theorem of finite difference schemes for IVPs, and finds its importance in characterization of convergent schemes [78].

Theorem 4.2.1. ***The Lax-Richtmeyer Equivalence Theorem.*** *A consistent finite difference scheme for a PDE for which the IVP is well posed is convergent if and only if it is stable.*

It is important to note that with the help of algebraic calculations, it is easy to verify the consistency and stability of the finite difference schemes. So using the equivalence part of the theorem, one can conclude the difficult result, convergence. In this work, we propose a finite difference based numerical implementation of the density and mass model developed in Chapter 2.

4.3 Formulation of Finite Difference Scheme

To construct the finite-difference method, we need to discretize the domain $[0, T] \times \Omega$. Here $\Omega = [a, b]$, a one dimensional domain. We introduce equidistributed grid points corresponding to a spatial step size h and to a time step k,

$$h = \frac{1}{N+1} \ , k = \frac{1}{M+1} \tag{4.43}$$

where M, N are integers, and define the grid points by

$$(x_i, t_j) = (ih, jk), \ \ i = 0, 1, 2, ...N+1, \ \ j = 0, 1, 2..., M+1. \tag{4.44}$$

Let $n(x, t)$ and $w(x, t)$ denote the exact solution of the system of equations (3.13) and (3.14). Then we denote the approximate solution at a point (x_i, t_j) by $(n_{i,j}, w_{i,j})$.

Now we refer to scheme (4.46) as the forward time and central space because forward difference and central difference approximations are used for the partial derivative terms

$$\frac{\partial n}{\partial t} \text{ and } \frac{\partial^2 n}{\partial x^2}, \tag{4.45}$$

respectively in equation (3.4).

$$\begin{aligned}\frac{n_{i,\,j+1} - n_{i,\,j}}{k} = a\ (1 - w_{i,\,j})\ &\frac{n_{i+1,\,j} - 2n_{i,\,j} + n_{i-1,\,j}}{h^2} \\ &- a\left(\frac{n_{i+1,\,j} - n_{i,\,j}}{h}\right)\left(\frac{w_{i+1,\,j} - w_{i,\,j}}{h}\right) \\ &\qquad + n_{i,\,j}w_{i,\,j}\,(1 - n_{i,\,j}w_{i,\,j}) - b\,n_{i,\,j}.\end{aligned} \tag{4.46}$$

Finite difference scheme (4.46) is used to track density of a population at a location x and time t. Now grouping the terms we get unknown density at the $(i, j+1)$th mesh point in terms of known values along the jth time level. This is called an explicit formula. Note: To calculate the values at the first time level, we have used the initial values at $t = 0$. The above scheme (4.46) can be further rewritten

$$\begin{aligned}n_{i,\,j+1} = z n_{i,\,j} &+ a\,r\,(1 - w_{i,\,j})\,(n_{i+1,\,j} - 2n_{i,\,j} + n_{i-1,\,j}) \\ &- a\,r(n_{i+1,\,j} - n_{i,\,j})(w_{i+1,\,j} - w_{i,\,j}) + k\,n_{i,\,j}w_{i,\,j}(1 - n_{i,\,j}w_{i,\,j}).\end{aligned} \tag{4.47}$$

Here a, b are the dimensional less rates defined previously in Section 3.2,

$$a = \frac{\mu}{\beta\,{L_m}^2}\ ,\quad b = \frac{d}{\beta} \tag{4.48}$$

and

$$r = \frac{k}{h^2}\ ,\quad z = 1 - b_1, \tag{4.49}$$

where

$$b_1 = \frac{kd}{\beta}. \tag{4.50}$$

Finite difference scheme (4.52) is referred as the forward time and forward space because forward difference approximations are used for the partial derivative terms

$$\frac{\partial w}{\partial t} \text{ and } \frac{\partial w}{\partial x}, \tag{4.51}$$

respectively in (3.5).

$$\begin{aligned}\frac{w_{i,\,j+1} - w_{i,\,j}}{k} &= a\ \,(1 - w_{i,\,j})\,\frac{1}{n_{i,\,j}}\Big(\frac{n_{i+1,\,j} - n_{i,\,j}}{h}\Big)\Big(\frac{w_{i+1,\,j} - w_{i,\,j}}{h}\Big)\\ &\quad + w_{i,\,j}\ (1 - n_{i,\,j}w_{i,\,j})\,(W_b - w_{i,\,j}) + c\ (1 - n_{i,\,j}w_{i,\,j})(1 - w_{i,\,j})\end{aligned} \tag{4.52}$$

Finite difference scheme (4.52) is used to track mass of a population at a location x and time t. Now grouping the terms, one can find the mass at the $(i, j+1)$th mesh point in terms of known values along the jth time level. This is also an explicit formula. Note: To calculate the values at the first time level, we have used the initial values at $t = 0$. This scheme (4.52) can further be simplified,

$$\begin{aligned}w_{i,\,j+1} &= w_{i,\,j} + r\ a\ \,(1 - w_{i,\,j})\,\frac{1}{n_{i,\,j}}(n_{i+1,\,j} - n_{i,\,j})(w_{i+1,\,j} - w_{i,\,j})\\ &\quad + k\ w_{i,\,j}(1 - n_{i,\,j}w_{i,\,j})\,(W_b - w_{i,\,j}) + c_1(1 - n_{i,\,j}w_{i,\,j})(1 - w_{i,\,j}).\end{aligned} \tag{4.53}$$

Here a, c denote the dimensionless rates defined previously in Section 3.2,

$$a = \frac{\mu}{\beta\, {L_m}^2}\ ,\quad c = \frac{\psi}{\beta} \tag{4.54}$$

and

$$r = \frac{k}{h^2}\ ,\quad c_1 = \frac{k\psi}{\beta}. \tag{4.55}$$

We have developed a finite difference scheme for the numerical solution to the system of coupled nonlinear partial differential equations arising from the modeling effort. In the following chapter, we will apply density and mass model to brown shrimp population in the Gulf of Mexico and demonstrate the use of the model.

5. APPLICATION OF DENSITY AND MASS MODEL TO GULF OF MEXICO BROWN SHRIMP FISHERY

Humans have fished for a long time, but over the past seven decades fisheries have grown at a much faster rate to meet the world's growing demand for seafood. Before the invention of technology for refrigeration, fishers caught a small amount of fish and preserved them using salting and drying, but with additional improvements in technology of processing and distribution, catch rates have increased [32, 65].

Fishery science started around the second half of 19th century when the fluctuations of fish stocks brought severe economic and political pressure in Europe [30,45,56]. So, scientists were hired in many countries to study population fluctuations. At the end of 19th century, scientists focused on tagging fish and study their migration patterns [13], earlier studies focus on understanding "where a fish was released " and "where it was recaptured", but the study provided a little information in between. In the early 20th century, a Norwegian scientist, Johan Hjort used a year class model and showed that changes in the survival rates cause fluctuations in abundance [32, 64]. But due to increased number and efficiency of fishing vessels, the fish caught became smaller and less abundant [32]. It is important to note that, efficiency of a year class model will be much more noticeable when the fishery is dependent on older year classes (four years) than younger year classes (two years) [70]. Later the halt in fishing during World war I resulted in bigger fish and higher catch [32, 53]. This provides some information on how scientists studied fluctuation of fish population, in the past.

The major breakthrough in finding the fluctuation of a fish population, came in the second half of 20th century when scientists from United states, England and Canada developed models (Surplus production models, yield-per-recruit models, age structured models) capturing dynamics of fish population [32, 35]. These models helped us to understand more about the potential causes of fish fluctuation and the effects of fishing pressure on fish abundance.

There has always been a boom and bust cycles in fisheries with many species [32,38]. This might be due to overexploitation when " too many fishers are chasing too few fish" [32] or it could be a part of natural fluctuations [39]. Fisheries are not always stable because as new stocks are exploited, fishers try to compete for more catch and profit. Environmental variability drives natural fluctuations in fish populations. For example, variations of the coupled ocean/atmosphere system known as El Nino-Southern Oscillation (ENSO) [4]. Within a few decades, fisheries may collapse due to overfishing [31, 32, 86]. Therefore, it is important to fish a population sustainably.

5.1 Shrimp Fisheries

According to a recent FAO report [11], the world's shrimp catch was estimated to be about 3.4 million tons per year, with Asia being its leading contributor (55% of the world catch). In light of its economic value, shrimp is one of the most important internationally traded fishery product. Shrimping industry provides jobs to millions of people across the globe (Table 6 in [11]).

There are two main types of shrimp fisheries that are operated in the United States of America, warm-water shrimp fisheries (Gulf of Mexico and southeast Atlantic coast) and the cold-water shrimp fisheries (northeast and northwest of United States of America). Gulf of Mexico shrimp fisheries target three major species of penaeid shrimp-brown shrimp (*Farfantepenaeus aztecus*), white shrimp ((*Litopenaeus setiferus*), pink shrimp (*Farfantepenaeus duorarum*).

Penaeid shrimp (warm water shrimps) are short-lived, essentially an annual crop, and have an ever changing size distribution with respect to its location [10]. Brown shrimp is the most important species harvested in the United States, and about 96% percent of the brown shrimp harvested in the United States in 2014 came from Gulf of Mexico, mainly from Texas and Louisiana [18, 21]. Shrimp fisheries are the highest valued fisheries in the southeastern United States (brown shrimp landings in 2014, 105 million pounds, valued at more than 305 million dollars). According to a recent 2015 stock assessment [28], the brown shrimp stock in the South Atlantic is not overfished and is not subject to overfishing.

5.1.1 Life History of Brown Shrimp (Farfantepenaeus aztecus)

Brown Shrimp spawn in deep waters (18-137m) throughout the year, with a major peak from February to March. Typically female lay 500,000 to 1 million eggs during its life time [18]. The eggs hatch within 24 hours of being fertilized [42]. The larval stage of Brown Shrimp lasts about 10-15 days. During this stage they are free-floating and thus cannot swim, but they control their vertical location within water column. When they grow about 2.5 mm long, they become opportunistic omnivores, feeding planktons and detritus. In the final larval stage, they are carried inshore to salt marshes and estuaries by tides and/or ocean currents.

The larvae primarily move at night, and are helped by incoming tides. Mortality at the postlarval stage is relatively high compared to later lifestages [51]. Over a 4-6 week period, the postlarvae transform to their juvenile stage [42]. Juvenile shrimp are vulnerable to size-dependent predation by fishes, birds, and other juvenile shrimp. Mortality from predation is thought to be one of the most prominent factor in regulation of recruitment of shrimp to fishery [51], but other factors may also control the recruitment [79].

Once they reach their sub-adult stage (50-66 mm), the shrimp begin to migrate offshore and become adults. As adults, shrimp live offshore 18-55 m below the surface and are demersal. They are most active at dusk and during the night. Like sub-adults, adults are omnivorous predators [42]. Brown shrimp are able to reproduce when they reach about 140 mm long. Most individuals die due to predation, other natural causes, or harvesting. Although some survive up to 2.5 years [42], a majority of them live up to approximately one year. Shrimp at all life stages serve as forage for pinfish, spotted seatrout, red drum, Atlantic croaker, southern flounder [52]. As a side note, brown shrimp's growth depends on factors such as water temperature and salinity [18].

5.2 Marine Protected Areas

The global perception of dwindling marine resources is triggering a call for more effective mechanisms to protect and conserve marine population [47, 55]. This has stimulated interest in and debate of the potential utility of "marine protected areas (MPAs)" as a tool for fisheries management. MPAs is one of the tools that has been increasingly used to protect and conserve marine population [61].

There are many different types of marine protected areas (MPAs) and marine reserve is one of them. Marine protected areas (MPAs) in the United States are defined as "any area of the marine environment that has been reserved by federal, state, territorial, tribal, or local laws or regulations to provide lasting protection for part or all of the natural and cultural resources therein", and are managed by the NOAA MPA Center [61]. Marine reserves is considered as a subset of marine protected areas [66], where in restrictions on some or all fishing activities are imposed. The term "marine reserve" means an area where some or all fishing are prohibited for a long period of time [61, 66]. This is also referred to as "no-take" reserve.

In the U.S., more than 1,700 MPAs have been established [50, 61], 41 % of all U.S. waters are in some form of MPA , while 3 % of all U.S. waters are highly protected marine reserves (no-take MPAs), to protect sensitive species and habitats [50, 62].

The majority of these MPAs focus on conserving critical marine habitat for fish and rebuilding stocks.

Our focus, in this dissertation will be on marine protected areas (MPAs) and how it could be used for protecting migratory species such as brown shrimp.

5.2.1 Background: Theoretical Studies on Marine Protected Areas

Literature on marine protected areas (MPAs) is abundant and has been growing very fast. Presently, studies on MPAs tend to focus on two main issues: benefits from establishing MPAs (in and outside the protected area) and the design of MPAs [60]. Even though the theoretical [5, 15, 33, 73] and empirical studies [6, 83] suggest that MPAs will benefit conservation of species, the debate on benefits of MPAs on the fisheries yields has been only discussed for little more than two decades [46].

Sanchirico and Wilen [73] consider a theoretical model with the density-dependent growth, and their results suggest that a protected area may increase the number of individuals of the population, in some cases may increase the sustainable yield. Movement of individuals from MPAs to fishing zones is termed “spillover” in fisheries. “Spillover” refers to the movement of adults and juveniles from MPAs into neighbouring fished areas, and the extent to which this occurs is dependent on the size of the zones, habitat configuration within them, and the abundance and mobility of the species [49]. Sanchirico and Wilen [73] also emphasise that when the spillover effect is significant, the MPAs could increase number of individuals outside the protected area.

Empirical studies of MPAs need a large amount of population data over different spatial and temporal scales, but such data are rarely available. This makes theoretical studies on marine protected areas very important. Berezansky [5] discusses the benefits of a theoretical modelling of MPAs, using a delay-differential model, and gives some insights into the type of fisheries data that should be collected in order to design

MPA. In a more recent article, Christou [15] uses Bioeconomic Ricker's model and concludes that greater profits under the optimal harvesting strategy was observed when the convergence to the optimal equilibrium solution was fast. Studies on theoretical bioeconomic models suggest that, increase in the average size of catch will result in an increase in demand value, and hence the higher market prices per unit of weight [68,73].

5.3 Parameters for Density and Mass Model

We now would like to demonstrate the utility of density and mass model developed in Chapter 2, of this dissertation. It is interesting to investigate how the migratory movement of brown shrimp population from MPAs to fishing zone affect the yield in the fishing area and whether the model is able to predict sustainability of brown shrimp outside the MPA. To answer these questions, one might have to parameterize the model and numerically simulate the model. The parameters for the model and their sources are shown in Tables 5.1 and 5.2.

Table 5.1: Instantaneous per capita rates for brown shrimp population

Per capita rates			
Symbol	Description	Value	Note
d	Natural instantaneous per capita mortality rate	3.3	[58]
β	Maximum instantaneous per capita birth rate	14	[58]
ψ	Maximum instantaneous per capita average growth rate	27	[12]

To calculate d, we have used a monthly natural mortality rate of 0.275 which was multiplied by 12 to obtain the annual rate [58]. For β , figure 10 from [58] was used. We fitted the Beverton-Holt curve, and obtained the maximum slope $(0.96 * 10^6)$, and finally took the natural log to convert from the finite rate to instantaneous rate. The value for ψ, we used data, daily rate of 0.074 g per day in [12] and was multiplied by 365 to convert to annual rate.

Table 5.2: List of parameters in the density and mass model

Parameter values			
Symbol	Description	Value	Note
K	Total biomass of parent stock per unit length	$6 * 10^7$	[27]
t	Time	1	Life cycle of shrimp 365 days
x	Domain length	1	Horizontal distance along the shore
L_m	Constant	0.1	Used to non-dimensionalize x

Now in the following section, we apply the density and mass model to brown shrimp population in Gulf of Mexico. In this dissertation, we will use three scenarios as a tool to demonstrate the use of density and mass model. First, we investigate the effects of marine protected areas on density and mass in and ouside the protected areas. Second, is to examine Instantaneous biomass yield and Sustainable biomass yield. In the third scenario, the importance of mass dependent per capita mortality and reproduction rates will be discussed.

5.4 Scenario 1: Marine Protected Areas

In this scenario, we divide the coastal line into discrete zones of marine protected areas and fishing zones. In this section, we assume 40% of the entire domain length is fishing zone under all models. Here the domain length is equivalent to the coastal line. Now having fixed the total fishing area to be 40 %, we start to allocate the network of MPAs. Starting with one fishing zone in the center, fishing zones spread like a wave reaching the ends of coastline, making up to 2^i fishing zones where $i = 0, 1, 2, 3, 4$, with equal width in each zone. The remaining 60% of domain length will be considered as the marine protected area. Except for the two fishing zone scenario, MPAs are equally distributed. Starting with there are two MPAs in one fishing zone scenario, MPAs spread like waves and reach corners of the coastal line, making $(2^i - 1)$ MPAs, where $i = 2, 3, 4$. The Table 5.3 shows the number and width of each fishing zone, number and width of MPAs.

Table 5.3: Number and width of fishing zone, and MPAs

Fishing Zones		MPAs	
Number	Width	Number	Width
1	4	2	3
2	2	3	2.5/1
4	1	3	2
8	0.5	7	0.86
16	0.25	15	0.4

We assume a hypothetical situation where density and mass of brown shrimp population is distributed by an initial profile as shown in Figures 5.1 and 5.2, respectively, along one dimensional coastal line.

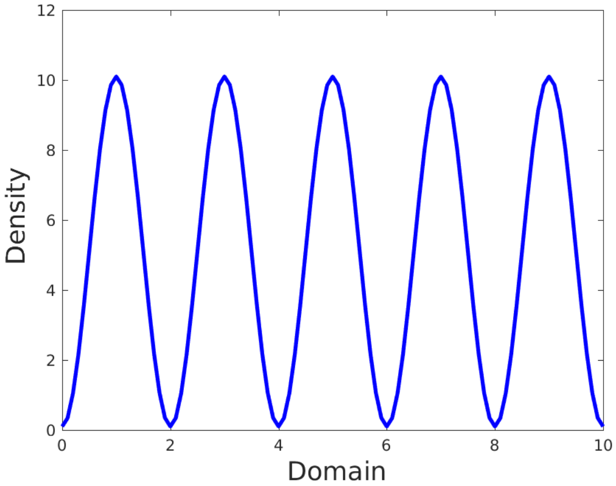

Figure 5.1: Hypothetical initial density of brown shrimp population distributed along coastal line

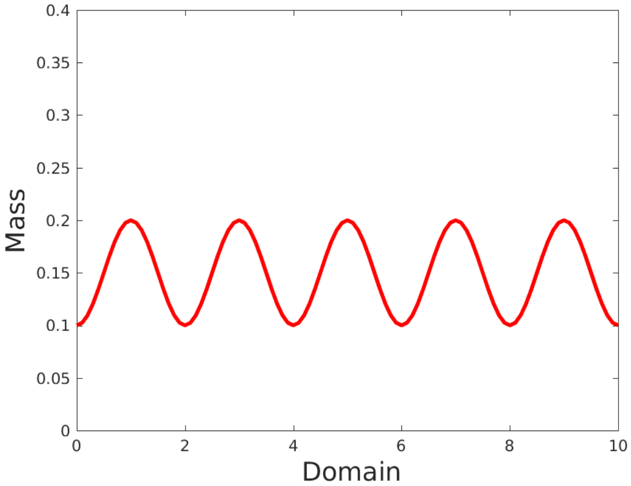

Figure 5.2: Hypothetical initial mass of brown shrimp population distributed along coastal line

In the following Subsection, we track the density and mass of brown shimp population, in and outside marine protected areas under different diffusive transport rates. It is interesting to investigate how the diffusive transport of population from the MPAs to the fishing zone affect the density and mass of the population. Table 5.4, shows different transport rates, used for numerical simulation.

Table 5.4: Low, medium and high diffusive transport rates

Diffusive Transport Rate μ_1	Value
Low transport	0.001
Medium transport	0.01
High transport	0.1

5.4.1 Results for Density and Mass in and outside Marine Protected Areas

Figures 5.3 and 5.4 depict asymptotic density and mass at large time $T = 100$, respectively in 2^i fishing zones where $i = 0, 1, 2, 3, 4$, with a maximum sustainable fishing rate under the ODE model, $f_S = 2.1$. The value for f_S was calculated using the equation (3.39) (Section 3.2). In this numerical computation, we have used $\beta = 14$, $\mu_1 = 0.001$ (Tables 5.1, 5.4) and let $d = 1.5$, $\psi = 2.5$. It is important to note that the qualitative results are the same when the values in the Table 5.1 were used for d and ψ, instead.

It is clear from the Figure 5.3 that the fishing pressure in the fishing zones brings down the numerical value of density and result can be compared to the results under the different diffusive transport rates μ_1 (Table 5.4). This result is in agreement with the real world situation that fishing pressure bring down the fish stocks [8] along the coastal line. From the Figure 5.3, it can be observed that density in MPAs have a high

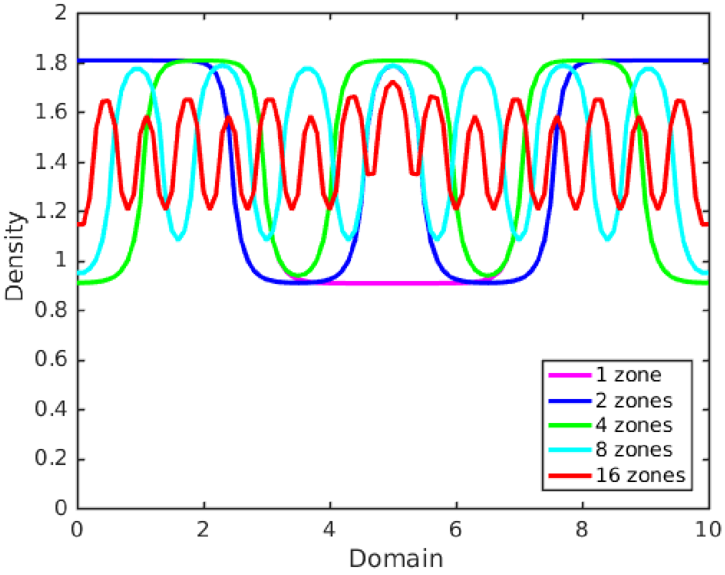

Figure 5.3: Asymptotic density of brown shrimp population with a transport rate $\mu_1 = 0.001$ under 2^i fishing zones where $i = 0, 1, 2, 3, 4$

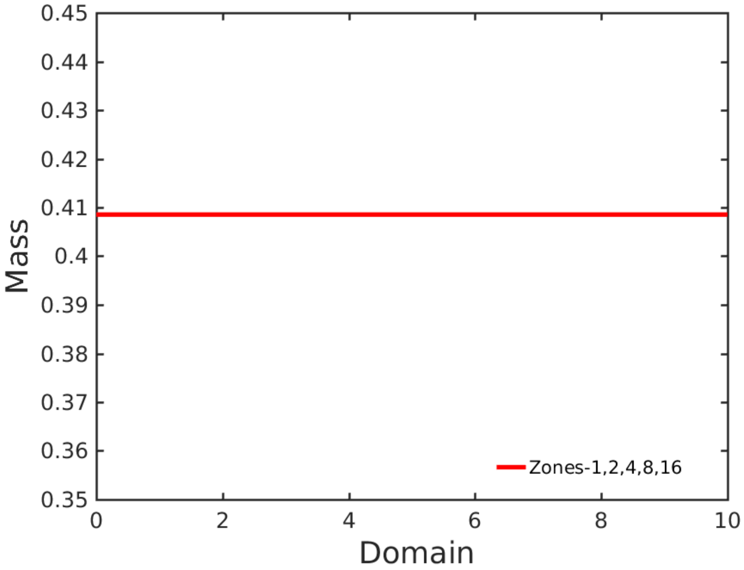

Figure 5.4: Asymptotic mass of brown shrimp population with a transport rate $\mu_1 = 0.001$ under 2^i fishing zones where $i = 0, 1, 2, 3, 4$

density gradient. Mathematically this is due to 1) the lower transport rate and 2) fishing rate is zero in MPAs, and ecologically this is due to a fewer number of individuals being transported from MPAs to fishing zones because of low mobility. Extremely low mobility is almost equivalent to sedentary fish in MPAs [33].

Mass aymptotes faster (compared to density) and remains constant (Figure 5.4), can be explained by the faster growth due to von Bertanffy type growth term in $G(n, w)$, expression (2.51).

Figures 5.5 and 5.6 depict asymptotic density and mass, respectively, at large time $T = 100$, in 2^i fishing zones where $i = 0, 1, 2, 3, 4$, with a maximum sustainable fishing rate under the ODE model, $f_S = 2.1$. The value for f_S was calculated using equation (3.39) (Section 3.2). The values for $\beta = 14$, $\mu_1 = 0.01$ were chosen from Tables 5.1, 5.4, respectively. We let $d = 1.5$, $\psi = 2.5$ because the qualitative results are the same when the values in the Table 5.1 were used for d and ψ, instead. The transport rate μ_1 for medium mobile species is 0.99% more than transport rate μ_1 for low transport. One can notice from the Figure 5.5 that the fishing pressure in the respective fishing zone brings down the numerical value of density and result can be compared to Figure 5.3. Higher aymptotic density in the fishing zones in Figure 5.5 can be observed; mathematically this is due to the effect of 1) higher transport rate (higher by 0.99%) and 2) lower gradient term in the marine protected areas and ecologically this is due to more spillover from MPAs.

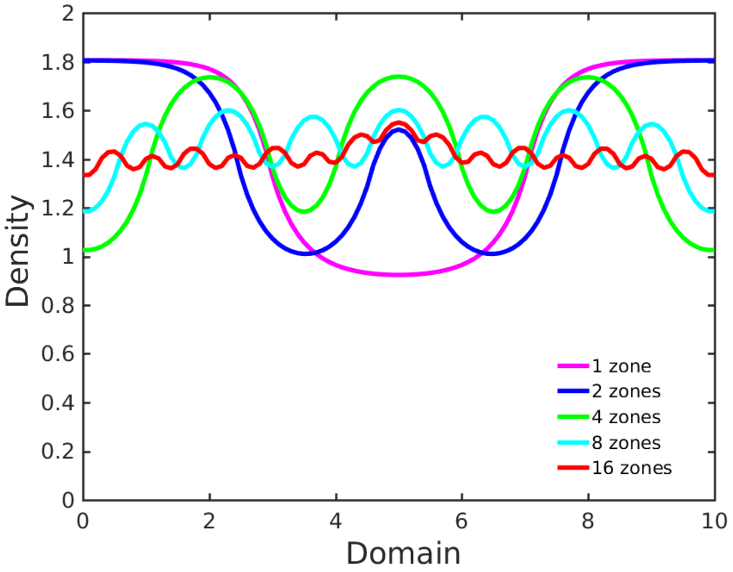

Figure 5.5: Asymptotic density of brown shrimp population with a transport rate $\mu_1 = 0.01$ under 2^i fishing zones where $i = 0, 1, 2, 3, 4$

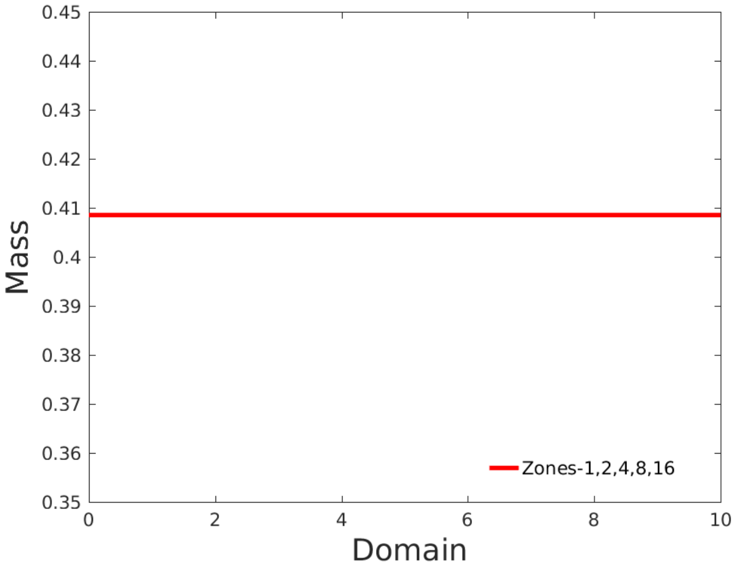

Figure 5.6: Asymptotic mass of brown shrimp population with a transport rate $\mu_1 = 0.01$ under 2^i fishing zones where $i = 0, 1, 2, 3, 4$

Figures 5.7 and 5.8 depict asymptotic density and mass at large time $T = 100$, respectively in 2^i fishing zones where $i = 0, 1, 2, 3, 4$ with a maximum sustainable fishing rate under the ODE model, $f_S = 2.1$. The value for f_S was calculated using equation (3.39) (Section 3.2). In the numerical computations, we have used $\beta = 14$, $\mu_1 = 0.1$ (Tables 5.1, 5.4) and let $d = 1.5$, $\psi = 2.5$. The transport rate μ_1 for highly mobile species is 9.9% more than transport rate μ_1 for medium transport. It is clear from the Figure 5.7 that the fishing pressure in the zone brings down the numerical value of density, and the result can be compared to Figure 5.5 where aymptotic density in the fishing zones is less when compared to the asymptotic density in the fishing zones for high transport Figure 5.7. One can observe that effect of gradient term in the MPAs almost smooths out due to the high transport rate, and ecologically this is due to a large number of individuals in MPAs being transported to the fishing zones due to high mobility.

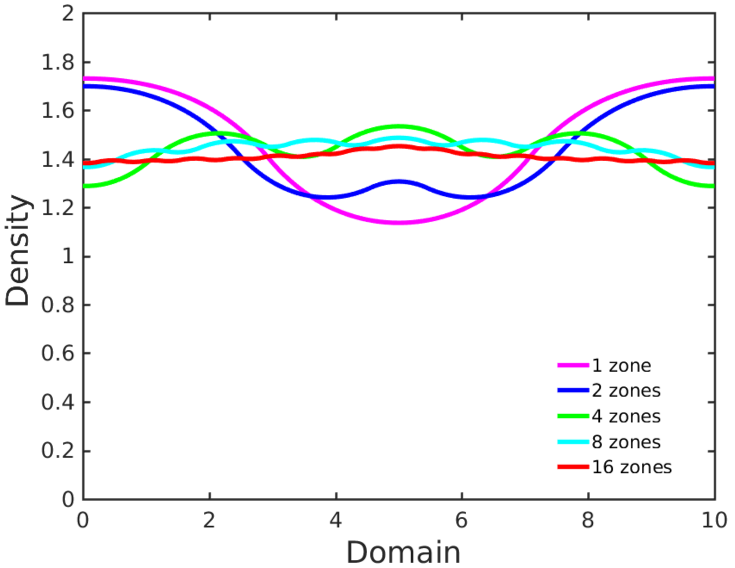

Figure 5.7: Asymptotic density of brown shrimp population with a transport rate $\mu_1 = 0.1$ under 2^i fishing zones where $i = 0, 1, 2, 3, 4$

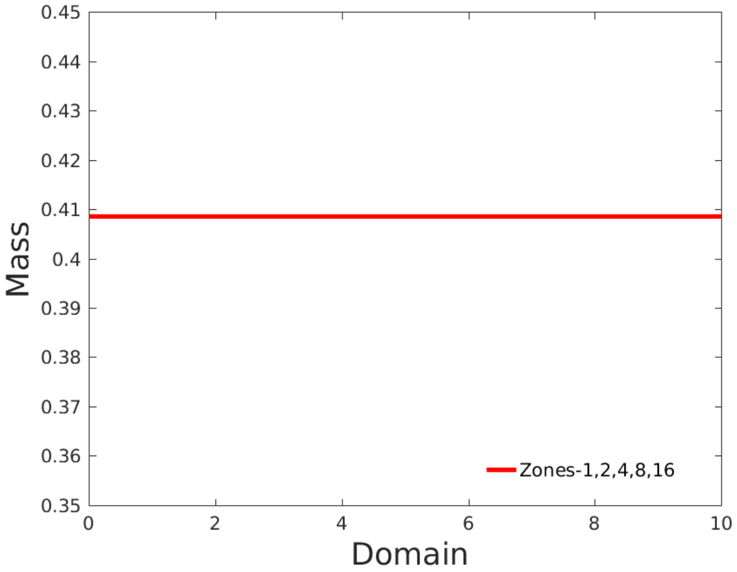

Figure 5.8: Asymptotic mass of brown shrimp population with a transport rate $\mu_1 = 0.1$ under 2^i fishing zones where $i = 0, 1, 2, 3, 4$

It is important to note that, mass approaches its asymptotic limit faster (compared to density) and remains constant (Figures 5.6, 5.8). This can be explained by the faster growth of shrimp and the von Bertanffy type growth term in the definition of nonlinear growth term $G(n, w)$, expression (2.51). The importance of mass in the density and mass model will be discussed later with Scenario 3, mass dependent mortality and reproduction.

The numerical results for density and mass of brown shrimp population from Scenario 1 will be used to explore biomass yield, which is more important for fisheries management. In particular, we try to investigate two different types of yield - Instantaneous and Sustainable biomass yield. Instantaneous and Sustainable biomass yield will be calculated for different transport rates (Table 5.4).

5.5 Scenario 2: Examine Instantaneous Biomass Yield and Sustainable Biomass Yield in Multiple Fishing Zones

In this section of the dissertation, we investigate Instantaneous biomass yield under multiple fishing zones and a network of MPAs. This section focuses on sustainability of fisheries yield.

Instantaneous biomass yield is the rate of change of catch (in weight) at each instant of time t. Sustainable biomass yield or the Equilibrium yield is the amount of biomass or harvested sustainably (i.e. asymptotic number density is positive) [63]. The following *Algorithm* presents a detailed description of calculation of Instantaneous biomass yield. The numerical solution for the density and mass model will be referred as solution matrix, that is, density matrix $n(t,x)$ and mass matrix $w(t,x)$. The column of a solution matrix represents the discrete points on the spatial domain (coastal line) and row of a matrix represents the time steps.

Algorithm 5.5.1

1. *From the solution matrices for density $n(t,x)$ and mass $w(t,x)$, we extract the columns where fishing takes place.*
2. *Multiply each cell of the extracted columns by the corresponding fishing rate **i.e.** f. Now we name the new matrix products as yield matrix.*
3. *Using the trapezoidal rule, yield matrix is integrated over x first, producing a column vector. The integral limits are the end points of corresponding fishing zone where the fishing happens.*
4. *Sum all integrated values (row wise), we get a column matrix of Instantaneous biomass yield.*

We use the Algorithm 5.5.1 to calculate the sustainable biomass yield. The asymptotic value of Instantaneous biomass yield is defined to be the Sustainable biomass yield.

5.5.1 Instantaneous Biomass Yield in One Fishing Zone

Figure 5.9 shows how coastline is divided into fishing zone and marine protected areas. From Figure 5.10, it can be observed that instantaneous biomass yield is a monotonically decreasing function of time as a result of the fishing with a maximum sustainable fishing rate under the ODE model, $f_S = 2.1$, (Section 3.2). Highest yield is observed in the case of higher transport rate μ_1, due to movement of individuals from MPAs to the fishing zone. As time progresses, instantaneous biomass yield approaches a constant value, which means that the yield is sustainable asymptotically.

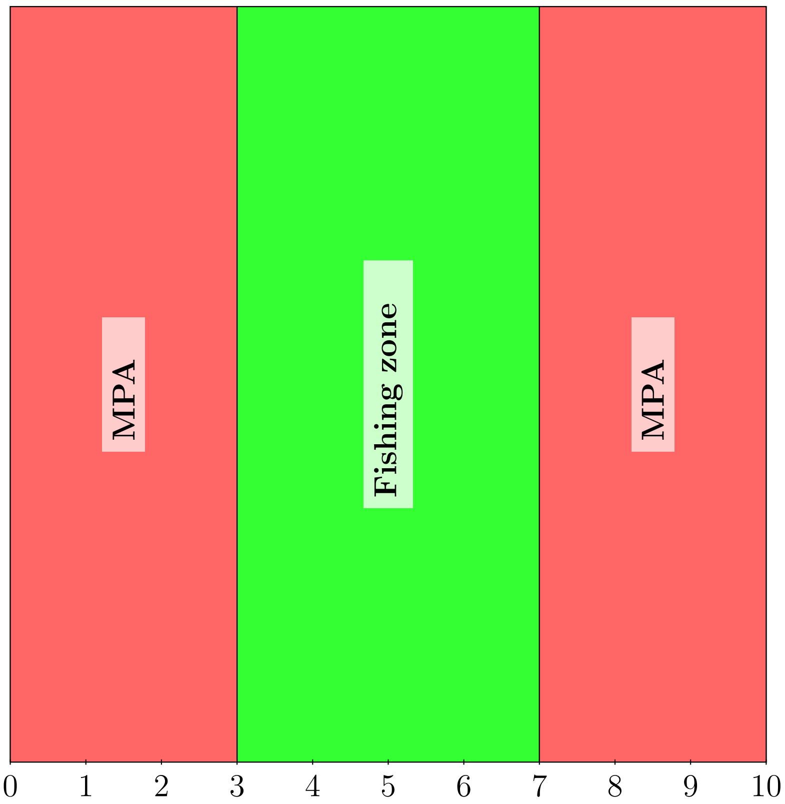

Figure 5.9: One fishing zone enclosing 40 % of total coastline area

Table 5.5: Instantaneous biomass yield for brown shrimp versus time in one fishing zone with low, medium, high transport rates

Large time	Instantaneous biomass yield		
T	Low Mobility	Medium Mobility	High Mobility
0	12.460001	12.460001	12.460001
2	7.737512	8.782985	9.771424
5	6.183391	7.074208	8.300134
10	4.319390	5.033029	6.655392
15	3.395595	4.096425	5.800939
20	2.928754	3.662593	5.4200210
40	2.340181	3.247472	5.174263

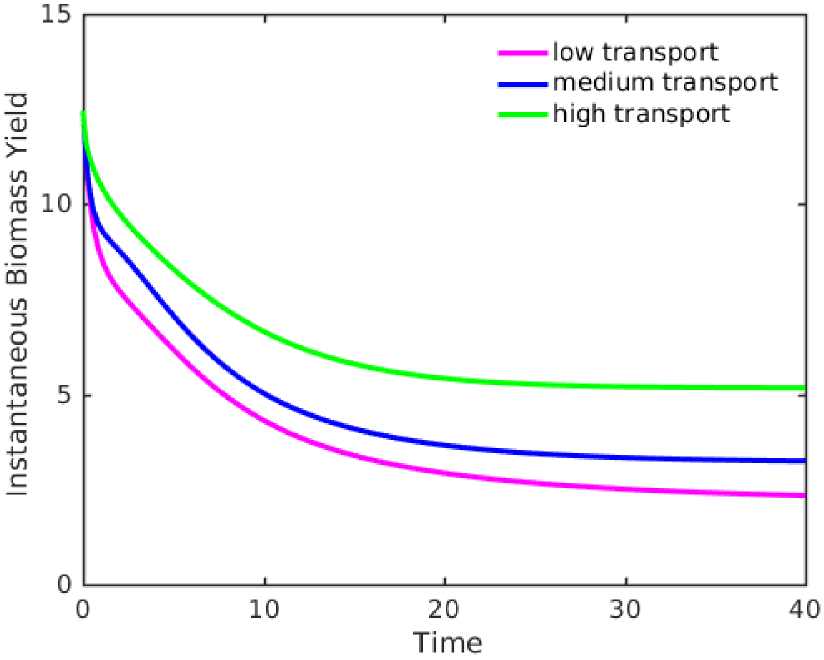

Figure 5.10: Instantaneous biomass yield versus time for brown shrimp with one fishing zone

5.5.2 Instantaneous Biomass Yield in Two Fishing Zones

Figure 5.11 shows how the coastline is divided into two fishing zones and three marine protected areas. From Figure 5.12, it can be observed that instantaneous biomass yield is monotonically decreasing function of time as a result of the fishing with a maximum sustainable fishing rate under the ODE model, $f_S = 2.1$, (Section 3.2). Secondly, one can observe the effects of higher yield when the transport rate μ_1 is increased. Table 5.6 shows by how much yield varies moving from low to high transport rate.

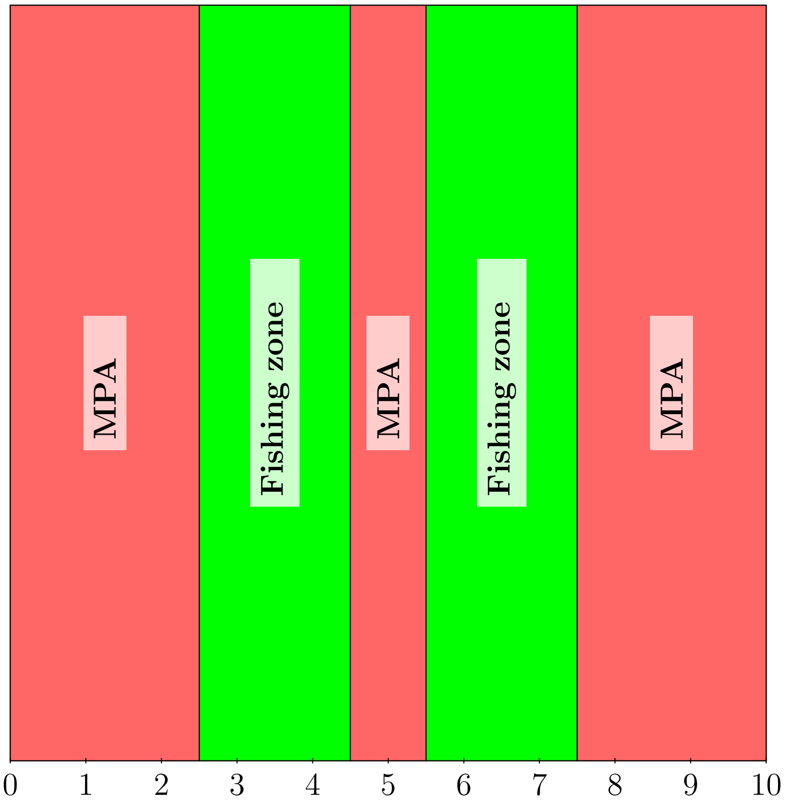

Figure 5.11: Two fishing zones enclosing 40 % of total coastline area

Table 5.6: Instantaneous biomass yield for brown shrimp versus time in two fishing zones with low, medium, high transport rates

Large time	Instantaneous biomass yield		
T	Low Mobility	Medium Mobility	High Mobility
0	20.796579	20.796579	20.796579
2	11.4059000	12.564359	14.113224
5	7.007028	8.347334	10.062939
10	4.461925	5.671389	7.297823
15	3.531309	4.717470	6.273090
20	3.089448	4.326083	5.872871
40	2.575297	4.037324	5.628824

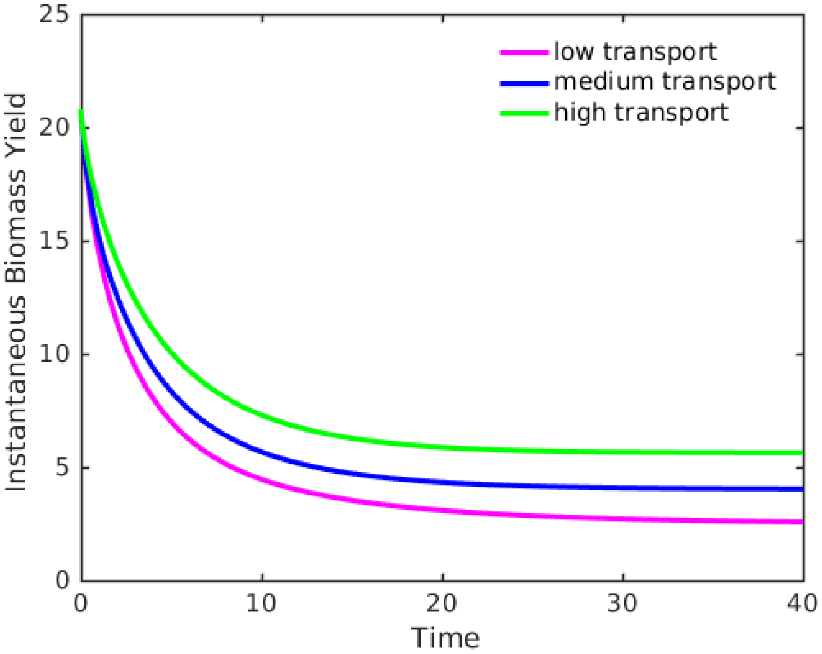

Figure 5.12: Instantaneous biomass yield versus time for brown shrimp with two fishing zones

5.5.3 Instantaneous Biomass Yield in Four Fishing Zones

Figure 5.13 shows how the coastline is divided into four fishing zones and three marine protected areas. From Figure 5.14, it can be observed that instantaneous biomass yield is monotonically decreasing function of time as a result of the fishing with a maximum sustainable fishing rate under the ODE model , $f_S = 2.1$, , (Section 3.2). Secondly, one can observe the effects of higher yield when the transport rate μ_1 is increased. Table 5.7 shows by how much yield varies moving from low to high transport rate.

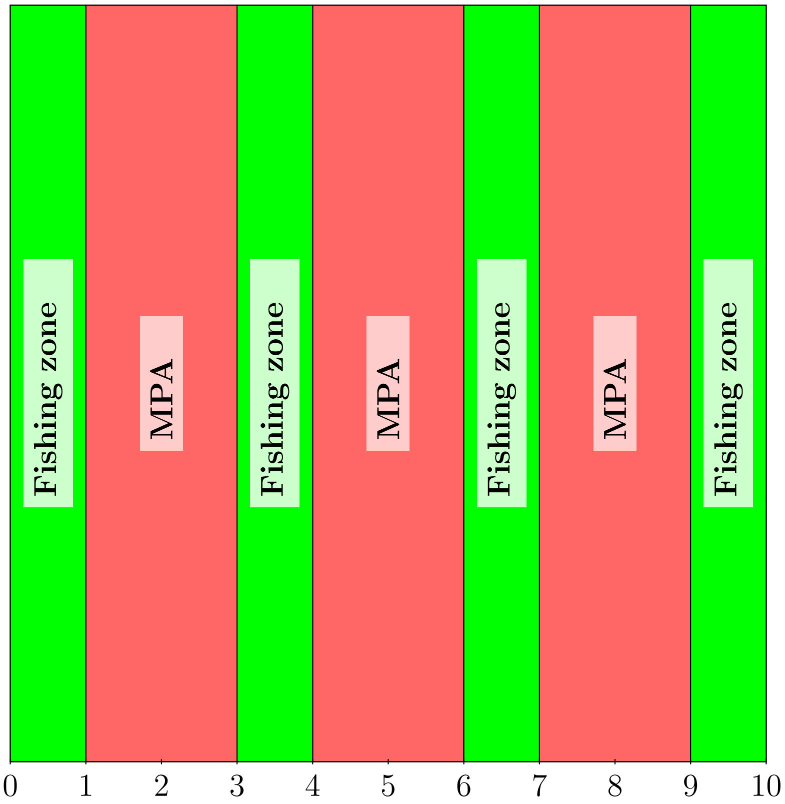

Figure 5.13: Four fishing zones enclosing 40 % of total coastline area

Table 5.7: Instantaneous biomass yield for brown shrimp versus time in four fishing zones with low, medium, high transport rates

Large time	Instantaneous biomass yield		
T	Low Mobility	Medium Mobility	High Mobility
0	12.284309	12.284309	12.284309
2	7.934292	9.202337	10.566509
5	6.427927	7.975846	9.3814400
10	4.643667	6.2742270	7.7447660
15	3.763726	5.4115880	6.888909
20	3.336219	5.0346960	6.5406260
40	2.889256	4.7861840	6.33943300

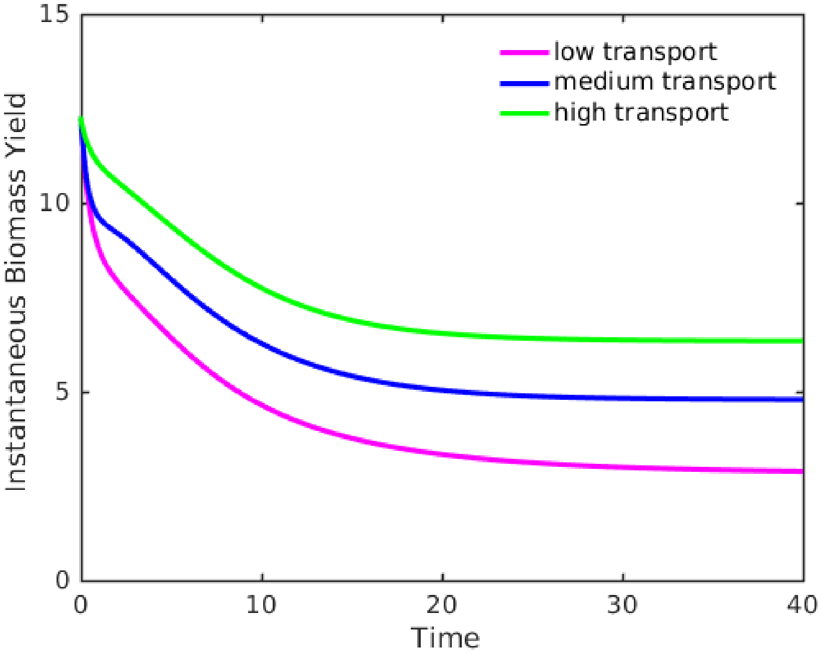

Figure 5.14: Instantaneous biomass yield versus time for brown shrimp with four fishing zones

5.5.4 Instantaneous Biomass Yield in Eight Fishing Zones

Figure 5.15 shows how coastline is divided into four fishing zones and three marine protected areas. From Figure 5.16, it can be observed that instantaneous biomass yield is monotonically decreasing function of time only for a low transport, with a maximum sustainable fishing rate under the ODE model , $f_S = 2.1$, , (Section 3.2). Yield is highest for high mobile species. After long time $T = 20$, instantaneous biomass yield tries to converge moving from medium to high transport. Table 5.8 shows by how much yield varies moving from low to high transport rate.

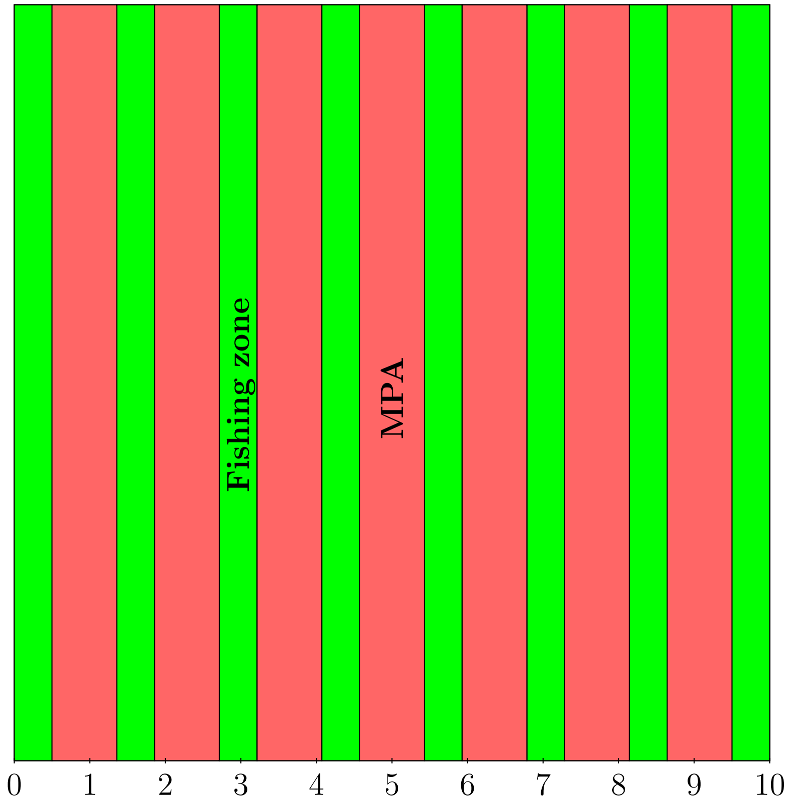

Figure 5.15: Eight fishing zone enclosing 40 % of total coastline area

Table 5.8: Instantaneous biomass yield for brown shrimp versus time in eight fishing zones with low, medium, high transport rates

Large time	Instantaneous biomass yield		
T	Low Mobility	Medium Mobility	High Mobility
0	10.690953	10.690953	10.690953
2	7.565422	9.788532	10.905982
5	6.8061480	9.209346	9.7385110
10	5.629434	7.641112	8.180111
15	4.9204340	6.762810	7.337824
20	4.558384	6.402698	6.982928
40	4.256985	6.200277	6.982928

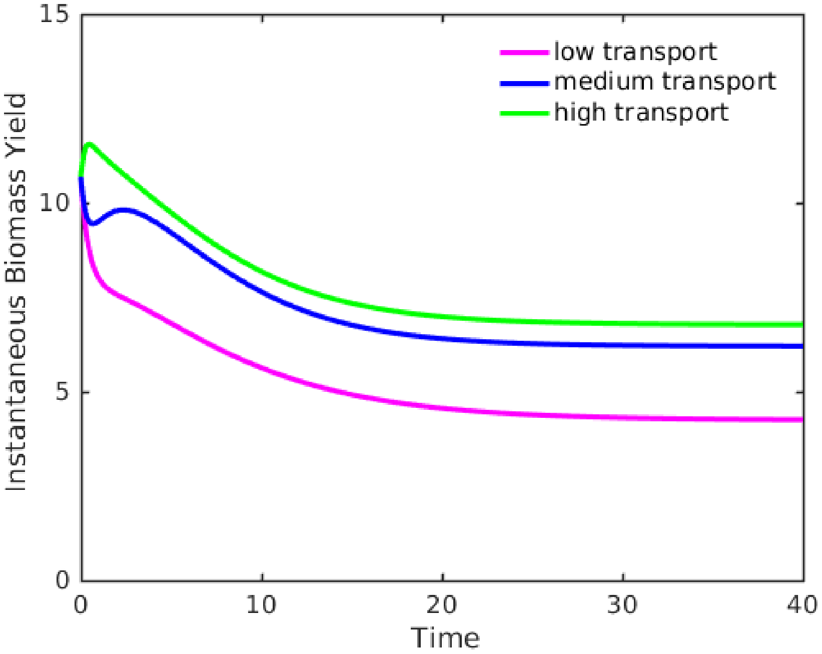

Figure 5.16: Instantaneous biomass yield versus time for brown shrimp with eight fishing zones

5.5.5 Instantaneous Biomass Yield in Sixteen Fishing Zones

Figure 5.17 shows how the coastline is divided into sixteen fishing zones and fifteen marine protected areas. From Figure 5.18, it can be observed that instantaneous biomass yield is monotonically decreasing function of time only for a low and high transport, with a maximum sustainable fishing rate under the ODE model, $f_S = 2.1$, (Section 3.2). Secondly, one can observe the yield is highest for high mobile species, Table 5.9. After long time $T = 20$, instantaneous biomass yield converges moving from medium to high transport.

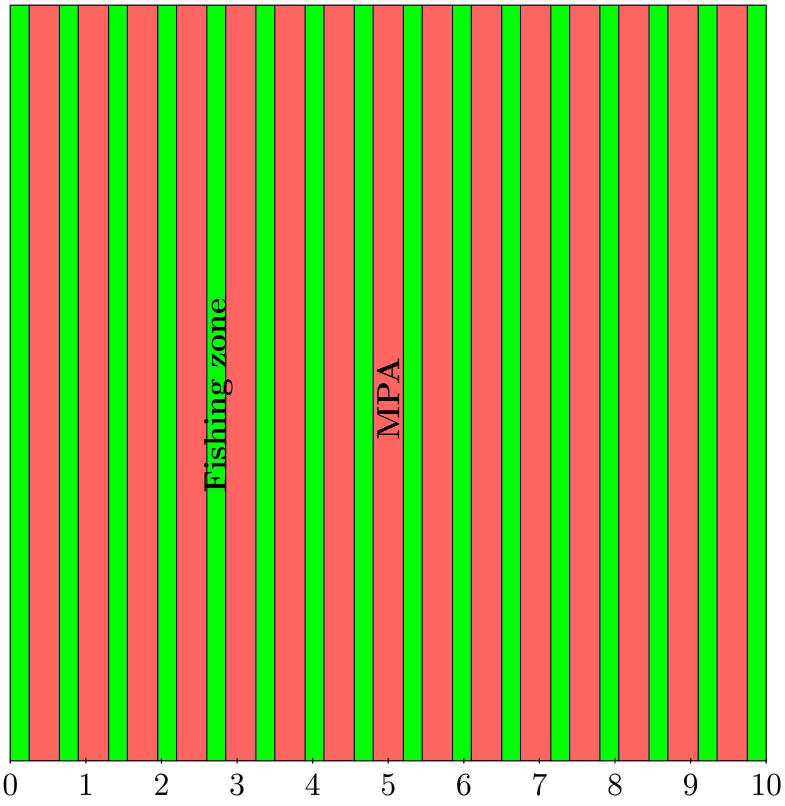

Figure 5.17: Sixteen fishing zones enclosing 40 % of total coastline area

Table 5.9: Instantaneous biomass yield for brown shrimp versus time in sixteen fishing zones with low, medium and high transport rates

Large time	Instantaneous biomass yield		
T	Low Mobility	Medium Mobility	High Mobility
0	11.956791	11.956791	11.956791
2	8.017647	10.140599	10.810734
5	7.808805	9.4227910	9.579765
10	6.859864	7.835784	7.95802600
15	6.1252320	6.9780760	7.097355
20	5.783410	6.6201000	6.733254
40	5.573617	6.4017030	6.507208

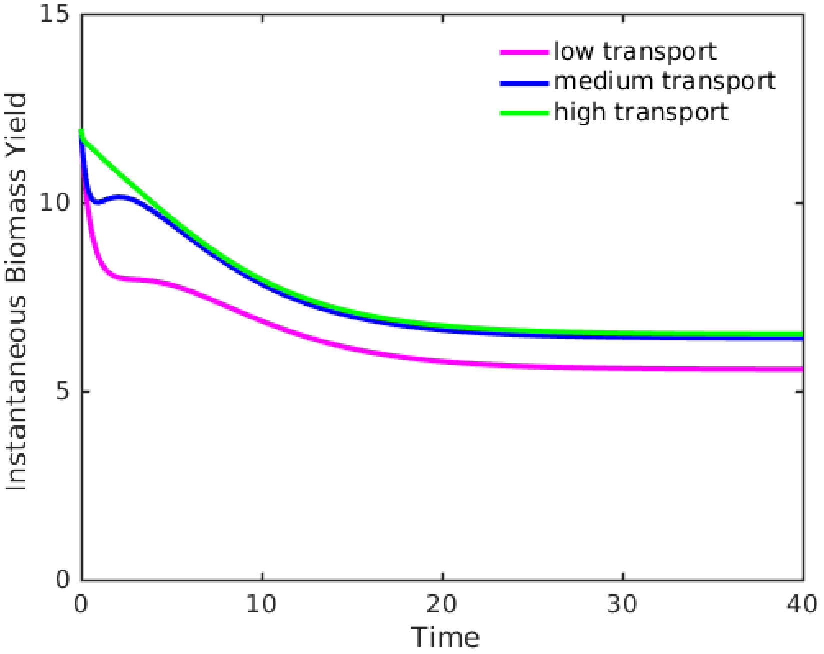

Figure 5.18: Instantaneous biomass yield versus time for brown shrimp with sixteen fishing zones

The results for instantaneous biomass yield, suggest that when we establish a network of marine protected areas along a coastline, starting from two MPAs in one fishing zone Scenario to fifteen MPAs in sixteen fishing zones Scenario, yield is always higher for a species with higher transport rate from the protected areas. The result is true for 2^i fishing zones where $i = 0, 1, 2,$(Figures 5.10, 5.12 , 5.14). Figures 5.16 and 5.18 suggest the convergence of yield for eight to sixteen zones when moving from medium to high transport. That is, yield converges as the number of fishing zones increase. The results for instantaneous biomass yield from the above discussion provides an insight to design of MPAs, it is crucial to consider the speed or mobility of species under consideration before MPAs are designed.

Results from the Scenario 1 suggest that with increase in the number of reserves, instantaneous biomass yield increases, which is consistent with several other existing results [47, 57]. Neubert [57], concludes no-take marine reserves are always part of an optimal harvest designed to maximize yield. Lubchenco and the authors in [47], analyze a large amount of literature from three major aspects (1) theoretical reserve design, (2) data used to parameterize the reserve models, and (3) practical application of reserve design, and conclude that networks of reserves is vital for longterm fishery and conservation benefits.

In this Section 5.5, how instantaneous biomass yield varies over time, under multiple fishing zones was observed. In the following Subsection we calculate sustainable biomass yield. An important aspect of sustainability, is "the assurity of the fish populations for the future".

5.5.6 Sustainable Biomass Yield with Different Mobility Rates

In this Subsection we present results for sustainable biomass yield of brown shrimp population with different mobility rates from marine protected areas. In particular, effect of MPAs on fisheries harvest will be explored. In fisheries, Maximum sustainable yield (MSY) is calculated, and fishery management policy is often determined based on MSY. MSY is the maximum catch that can be caught without depleting the population. Though the goal might be to optimize the yield, it is always ideal to set the yield below the MSY to take precautionary approach. To ensure a sustainable harvesting, there must be a balance between birth, death, and growth.

We define high intensity fishing rate f_I,

$$f_I = \frac{f_S}{\left(\frac{Fishing_{area}}{Total_{area}}\right)} = \frac{f_S}{0.4}, \tag{5.1}$$

where f_S is the maximum sustainable fishing rate without any movement of individuals over space.

The fishing rate within a fishing zone which gives MSBY, (over the entire space) in a PDE model is denoted by $f_S^{'}$. We have chosen a wide range of fishing rates $f_S^{'}$,

$$0 \leq f_S^{'} \leq 2\ f_I, \tag{5.2}$$

including fishing rates below f_S, at f_S, and above f_S, where f_S is the maximum sustainable fishing rate f_S (equation 3.39).

From the Figure 5.19, it can be observed that for a lower transport rate, with 2^i fishing zones, where $i = 0, 1, 2$, the yield declines with increase in the fishing rate and with increase in the number of fishing zones. It is necessary to note that when we increase the number of fishing zones, the size of fishing zone becomes smaller. This, in turn, reduces the size of MPAs (Table 5.3). Whereas for 2^i fishing zones, where $i = 3, 4$, yield goes up and is sustainable, with increase in the fishing rate and with increase in the number of fishing zones. Our numerical results for low transport rate suggest that in a multiple fishing zone scenario with a network of MPAs, small MPAs (width 0.4) is effective in producing sustainable yield for low mobile species. Our results are consistent with the study in reef habitats [71], where many species are relatively sedentary (low mobility). They conclude relatively small protected areas can provide good protection.

Maximum sustainable biomass yield (MSBY) in absence of marine protected areas occur at a maximum sustainable fishing rate , $f_S = 2.1$, as discussed in Section 3.2. But when a network of marine protected areas are designed along the coastline, Figure 5.19 shows that the fishing rate at MSBY increases with the increase in number of fishing zones and number of marine protected areas. This suggests that fishing rate outside the MPA should be adjusted to reach MSBY.

Table 5.10: Sustainable biomass yield for brown shrimp with low mobility from MPAs for wide range of fishing rates

Fishing rates	Sustainable biomass yield for brown shrimp				
	One Zone	Two Zones	Four Zones	Eight Zones	Sixteen Zones
0.7	1.730568	1.734707	1.741538	1.784138	1.842206
1.4	2.795469	2.815708	2.847701	3.033704	3.267429
2.1	3.205285	3.262787	3.348913	3.804634	4.325931
2.8	2.980892	3.116243	3.303159	4.174506	5.073841
3.5	2.178531	2.477112	2.830268	4.245470	5.570251
4.2	1.129321	1.657743	2.187961	4.136744	5.873084
4.9	0.670693	1.147688	1.706765	3.955198	6.034800
5.6	0.548144	0.913793	1.417482	3.764675	6.099261
10.5	0.348950	0.501663	0.7949210	2.956080	5.725805

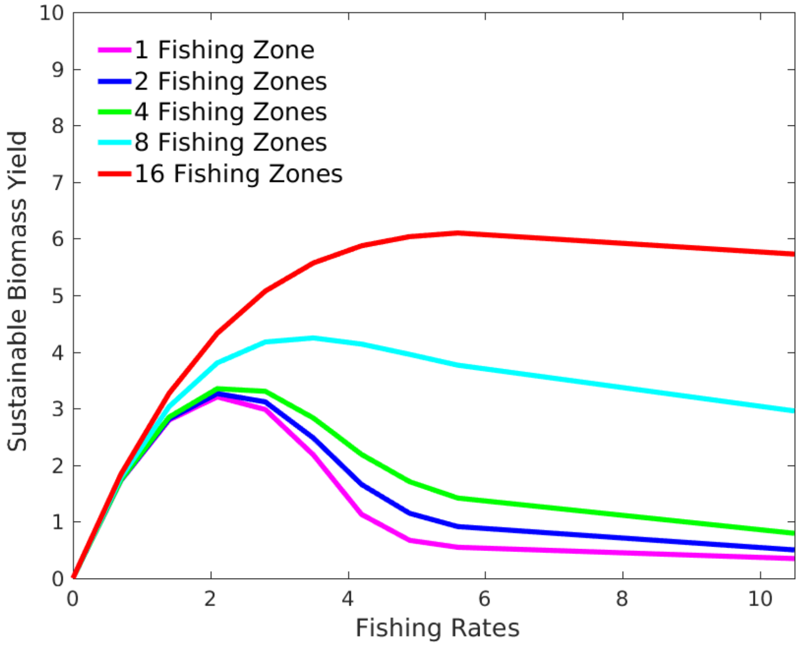

Figure 5.19: Sustainable biomass yield for low mobile species

The results for the medium transport rate suggest that fishing rate at MSBY under the PDE model changes. That is, the maximum sustainable fishing rate f_S at MSBY occurs, gets shifted from 2.1 in one fishing zone scenario to 5.6 in eight fishing zones scenario. Secondly, it can be observed from figure 5.20, sustainable yield declines with increase in fishing rates under 16 fishing zones. The results from [83] suggest that for a relatively mobile species, large number of small MPAs are not effective. Our result also suggest the same. It is clear, and possibly expected, that the transport of individuals from the marine protected area to the fishing zones is adding number of individuals at a faster rate for medium mobile species. This accounts for MSBY in 2^i fishing zones, where $i = 0, 1, 2, 3$, for medium transport species (compared to low transport species).

Table 5.11: Sustainable biomass yield for brown shrimp with medium mobility from MPAs for wide range of fishing rates

Fishing Rates	Sustainable biomass yield for brown shrimp				
	One Zone	Two Zones	Four Zones	Eight Zones	Sixteen Zones
0.7	1.753978	1.777618	1.806458	1.878390	1.90050
1.4	2.899695	3.004482	3.1247600	3.40311700	3.478412
2.1	3.471653	3.732666	4.0106430	4.607401	4.7456000
2.8	3.533471	4.038750	4.534864	5.52656700	5.714287
3.5	3.210255	4.027124	4.78123000	6.1971890	6.3970720
4.2	2.723971	3.819868	4.8377000	6.6558620	6.8069750
4.9	2.307941	3.529529	4.7819960	6.93779000	6.957522
5.6	2.030675	3.232480	4.670519	7.075454	6.862914
10.5	1.431415	2.015941	3.8268200	5.9360760	1.684389

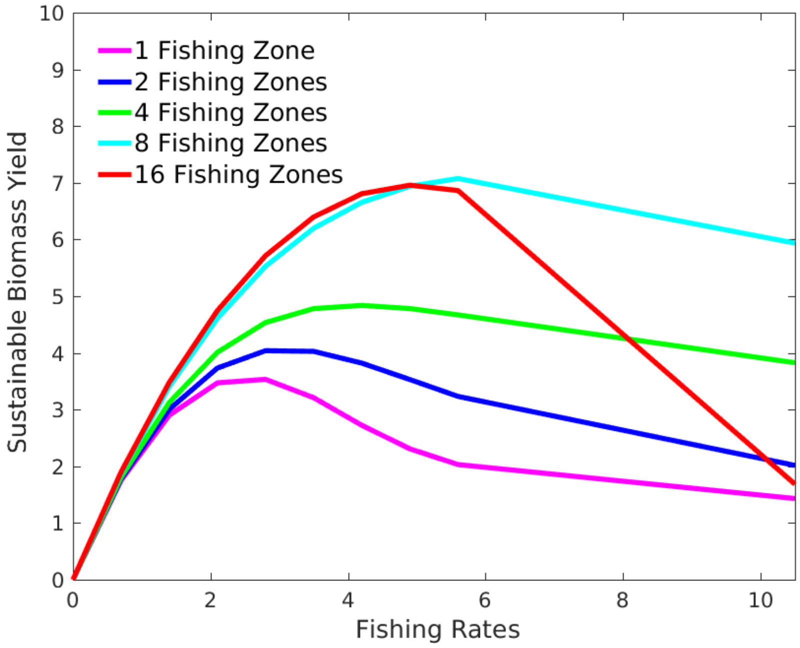

Figure 5.20: Sustainable biomass yield for medium mobile species

Figure 5.21 depicts the sustainable yield for highly mobile species. The maximum sustainable fishing rate at MSBY is shifted from 4.9 in one fishing zone scenario to 5.6 in eight fishing zones scenario. Secondly, it can be observed from figure 5.21, sustainable yield declines at a higher fishing rate ($f > f_I$), with increase in number of fishing zones and large number of small MPAs, for 2^i fishing zones, where $i = 2, 3, 4$. Again our results are consistent with results from [83], for a relatively mobile species, large number of small MPA's are not effective.

Table 5.12: Sustainable biomass yield for brown shrimp with high mobility from MPAs for wide range of fishing rates

Fishing Rates	Sustainable biomass yield for brown shrimp				
	One Zone	Two Zones	Four Zones	Eight Zones	Sixteen Zones
0.7	1.823057	1.853153	1.890472	1.919047	1.911459
1.4	3.191918	3.303016	3.445484	3.549009	3.515612
2.1	4.161546	4.386079	4.688360	4.896255	4.814192
2.8	4.797125	5.144227	5.643471	5.967356	5.809044
3.5	5.170131	5.624508	6.335924	6.769108	6.502180
4.2	5.351554	5.877973	6.791159	7.308557	6.895842
4.9	5.404406	5.957286	7.034499	7.593034	6.992606
5.6	5.378536	5.913185	7.090663	7.630203	6.795569
10.5	4.773903	4.786750	4.043021	2.024522	0.239171

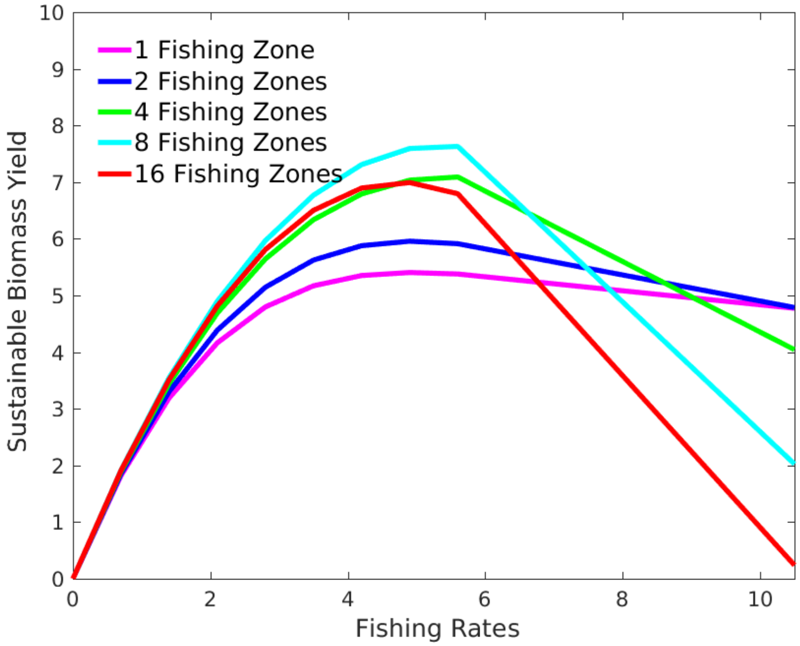

Figure 5.21: Sustainable biomass yield for highly mobile species

The numerical results from Scenario 2 suggest that for a low mobile species when (1) fishing rate is increased and (2) increasing the number of fishing zones (decreasing the size of fishing zones/MPAs) (Table 5.3), yield is sustainable. On the other hand for a medium and high mobile species at higher fishing rate ($f > f_I$), yield declines with (1) increase in fishing rate and (2) increase in the number of fishing zones. So this suggests that there is a need to identify the mobility of species before implementing MPA. The result also gives insight on the size of MPAs relative to mobility of species.

Results from [57] suggest that the optimal harvesting strategy is a spatial "chattering control" with infinite sequences of reserves alternating with areas of intense fishing. These results are inconsistent with the results in above discussion (Section 5.2). Results from Scenario 2, suggest that sustainable yield increase/decrease with the increase in the fishing rate.

Kaplan [33] uses a stage structure model and compares the change in average individual biomass with the change in individual lifetime reproduction due to increasing reserve area. The author concludes that maximum sustainable yield (MSY) increases with size of MPAs. Our results from Scenario 2 suggest that for the medium and high transport species, for $i = 1, 2, 4$, in 2^i fishing zones, MSBY increases with large MPAs.

Kaplan [33] also discusses many other modeling studies on how MPAs affect fisheries harvest [26, 29]. A few of them will be discussed here, since the results from these models can be compared with the results from Scenario 2. (1) Hastings [29] uses a simple two stage (source and sink) model and he suggests that MSY is same with and without reserves in simple models. (2) Hart [26] suggests that MSY changes with implementation of reserves. That is, when size structure is added to model, harvesting rate can be changed to maximize yield. Our model includes size structure, network of MPAs and suggests that yield changes with and without reserves.

In this section, the effects of marine protected areas (MPAs) on fisheries harvest was investigated. The density and mass model and vital rates - transport , mortality, growth, reproduction, were used to determine the best harvesting strategy that produces Maximum Sustainable Biomass Yield (MSBY) with a network of MPAs.

5.5.7 Sustainable Biomass Yield for a Wide Range of Fishing Rates

In this Subsection, we use the numerical results obtained in the above Subsections 5.4.1, 5.5.2-5.5.6 to determine the harvest rate that produces MSBY under different diffusive transport rates. One might often see large scale fluctuations in fish population and fisheries stock collapse [56]. There may be several factors for such collapse: for example, environmental conditions, and high harvesting rates. One of major reason for collapse is high harvesting rate. Hence it is crucial to apply a harvest rate that ensures the sustainability of a population. The results from the scenario 2 indicates the importance of knowing the spatial explicit harvesting strategies.

From the Figures 5.22 - 5.30, it can be observed that how sustainable biomass yield varies with respect to number of fishing zones, for a fixed value of fishing rate under different diffusive transport rates. In particular, figure 5.30, suggests that population collapses with increase in the number of fishing zones under high fishing rate when the species are highly mobile. Tables 5.10, 5.11, 5.12 were used to plot sustainable biomass yield versus fishing zone for a fixed value of fishing rate.

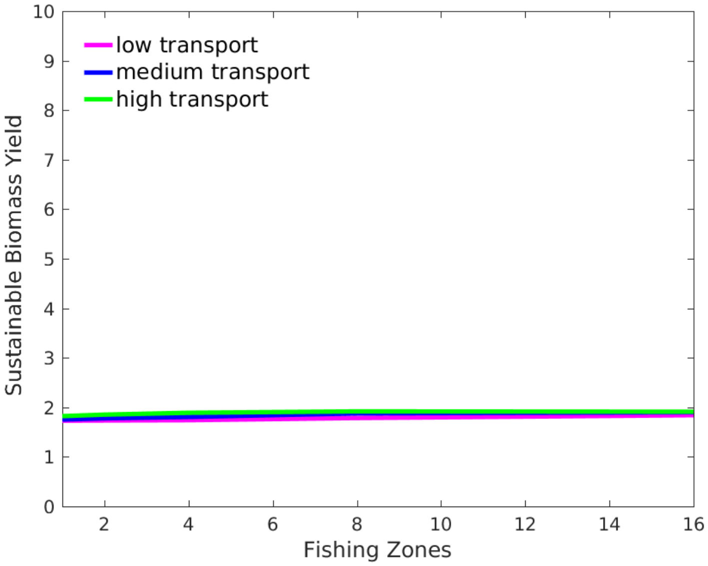

Figure 5.22: Sustainable biomass yield for fishing rate f=0.7

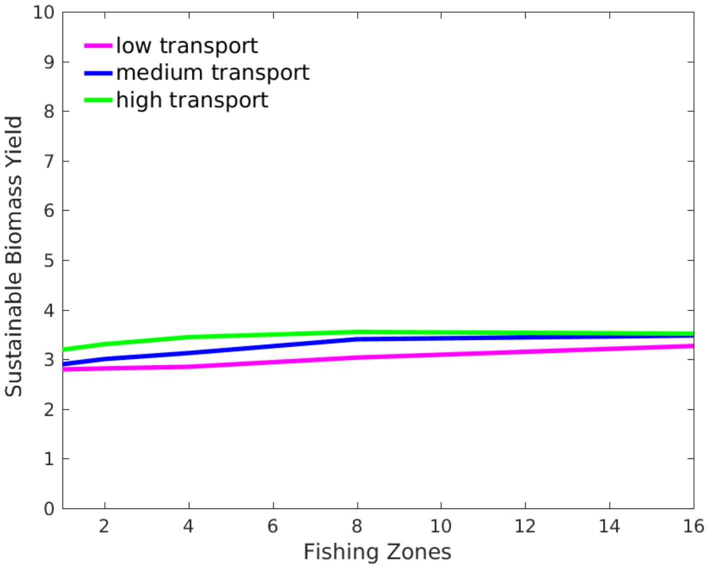

Figure 5.23: Sustainable biomass yield for fishing rate f=1.4

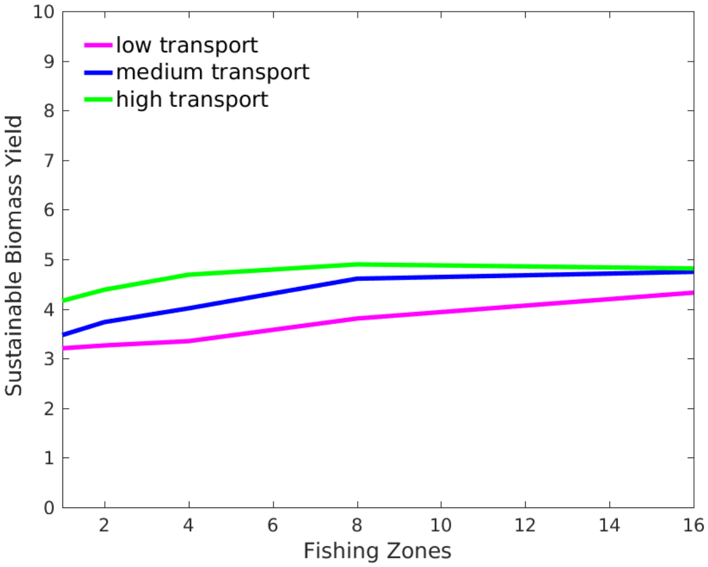

Figure 5.24: Sustainable biomass yield for fishing rate f=2.1

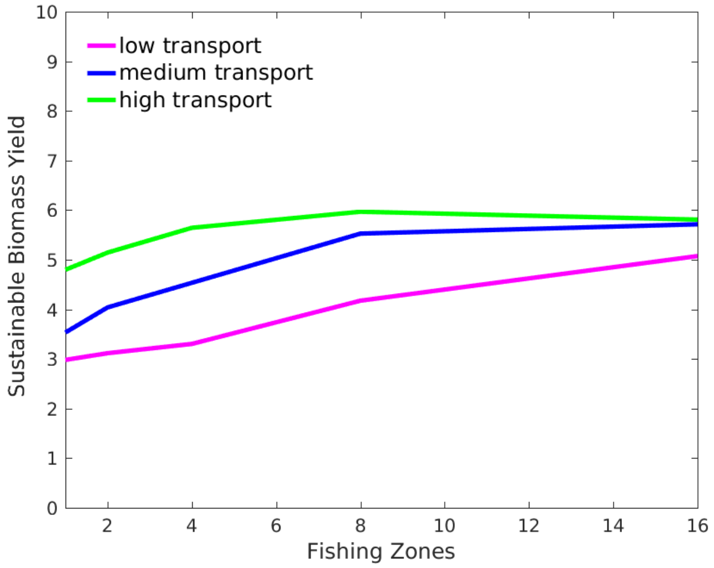

Figure 5.25: Sustainable biomass yield for fishing rate f=2.8

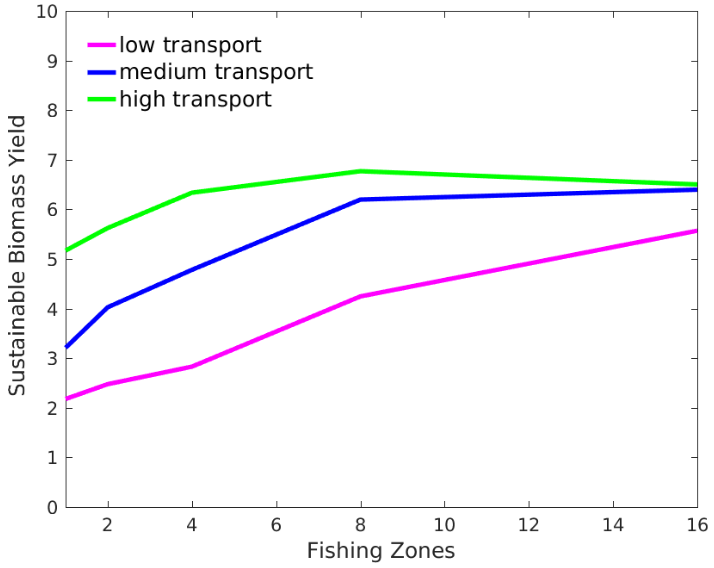

Figure 5.26: Sustainable biomass yield for fishing rate f=3.5

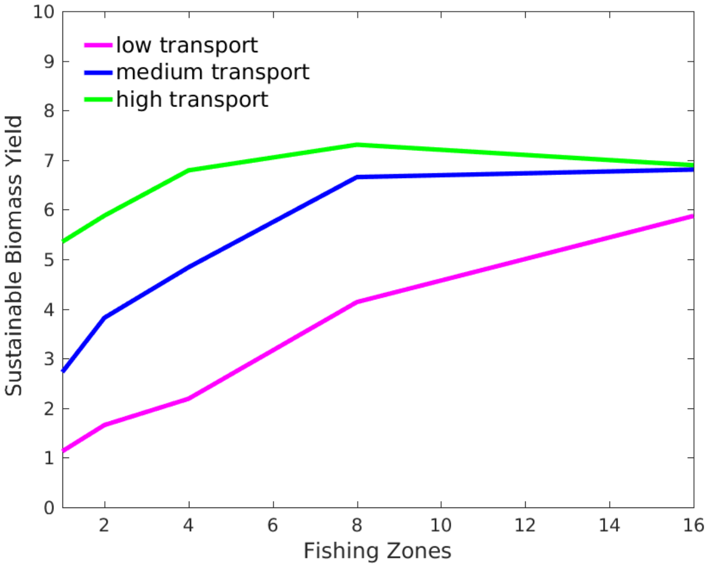

Figure 5.27: Sustainable biomass yield for fishing rate f=4.2

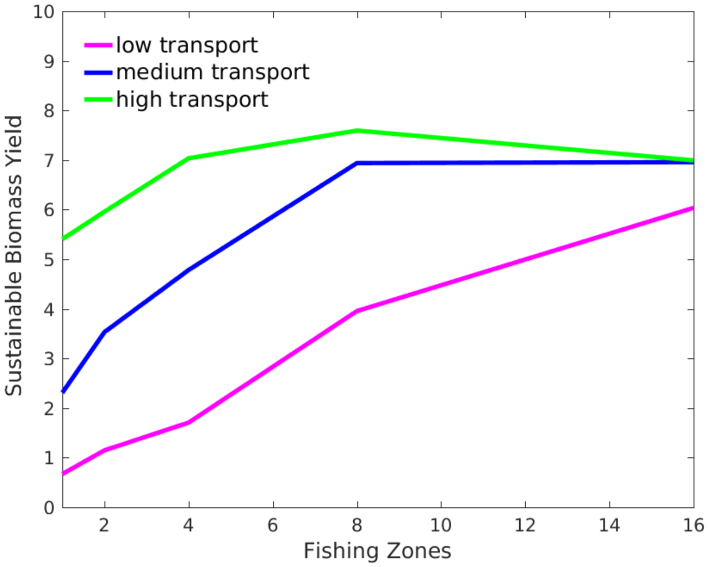

Figure 5.28: Sustainable biomass yield for fishing rate f=4.9

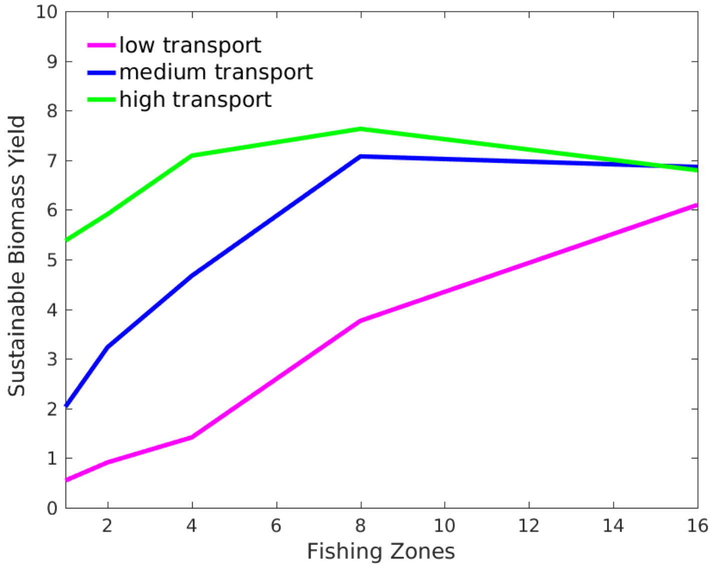

Figure 5.29: Sustainable biomass yield for fishing rate f=5.6

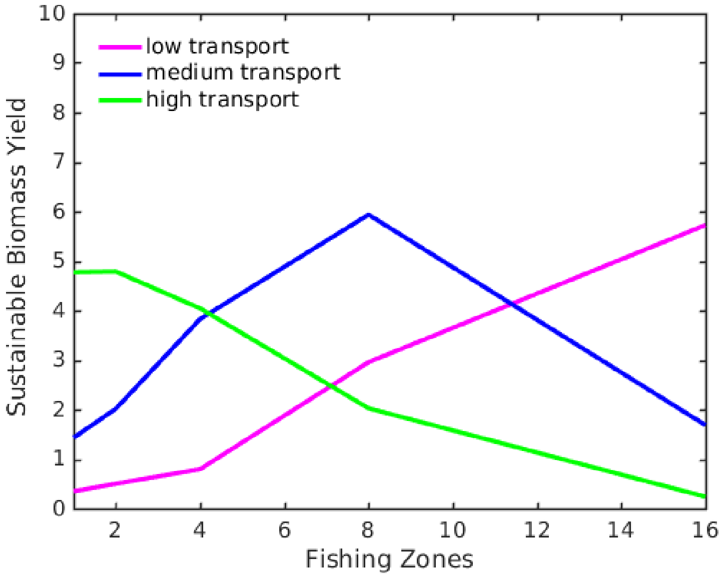

Figure 5.30: Sustainable biomass yield for fishing rate f=10.5

5.5.8 Discussion Leading to a Conjecture

Conjecture 1. For a low mobile species, when (1) fishing rate is increased and (2) increasing the number of fishing zones, biomass yield is sustainable. However, for a medium and high mobile species, when fishing at higher rate ($f > f_I$), biomass yield declines with (1) increase in fishing rate and (2) increase in the number of fishing zones.

Ecological reasoning. Transport of species from MPA to fishing zone sustains the population in fishing zone.

There is significant positive effect of protected areas on abundance, size, and density inside the MPA [48, 72]. When low mobile species are inside the MPA, they tend to remain inside. Then the time spent inside the protected area is more, they have more opportunity to grow larger and larger individuals reproduce more offspring [48], adding sustainability of the population in the case of low mobile species.

For medium and high mobile species at higher fishing rates ($f > f_I$), the biomass yield declines with increase in the fishing rate, increase in the number of fishing zones due to low asymptotic density (in and outside MPA) compared to low mobile species, (Figures 5.5 and 5.7). This can be explained by species movement, species move in and out of MPA at a faster rate. Due to the faster movement, chances of being caught by fishers are more. In turn there are fewer fish in the protected area.

The main result of this Section 5.5, suggest that -"low mobile species show sustainability " with the increase in the number of fishing zones under high fishing rate ($f > f_I$), and large number of small protected areas.

In the following section, we would like to investigate mass dependent natural mortality in our model. Mortality of smaller individuals are more when they are young. But as they grow, natural mortality decreases.

5.6 Scenario 3: Mass Dependent - Mortality and Birth

To understand the trade-off between density and mass of brown shrimp in Gulf of Mexico, we make two important biological processes, mortality and reproduction, mass dependent. Importance of mass was discussed in Chapter 1 of this dissertation. Mass in this study means the average mass, as defined previously in Chapter 2, Section 2.1.

Mass dependent mortality tells us that the chance of survival is higher with increase in mass. Studies show that in many of the marine species survival rate of larger individuals are more than the smaller ones [1]. Birth affects the number of individuals in a population. In the case of mass dependent birth rate, instantaneous birth rate is a function of average mass. Mass dependent birth incorporates an important biological process that birth increases with body mass, *i.e.* larger individuals tend to produce more offspring.

We would like to see the effect of these two types of mass dependence on density and mass of brown shrimp population. To understand the mass dependency, we consider three cases given in Table 5.13.

Table 5.13: Mass dependent/Constant per capita rates

Case	Natural mortality d	Instantaneous birth rate β
I	$d(w)$	$\beta(w)$
II	$d(w)$	β
III	d	$\beta(w)$

We define mass dependent natural mortality as

$$d(w) = d_{min} + (w_m - w)\frac{d_{max} - d_{min}}{w_m - W_b}. \tag{5.3}$$

Here w_m is the "maximum mass" an individual can attain, and W_b is the non dimensional birth mass,

$$W_b = \frac{w_b}{w_m}, \tag{5.4}$$

where w_b is the birth mass. d_{min} and d_{max} are the minimum and maximum natural mortality rates, respectively. Initially, we assume a low initial mass in a population, that is, a population consists of small individuals. Mathematically this means, when w is close to W_b, then mass dependent mortality $d(w)$ takes d_{max} as its value. Ecologically, natural mortality is often higher when an individual is smaller in size [51]. But when an individual grows in size, that is when w approches w_m, mass dependent mortality $d(w)$ approaches d_{min}. The nonlinear reaction diffusion-hyperbolic PDE will be used for examining the mass dependent rates.

$$\frac{\partial n}{\partial t} = \mu_1 \left(1 - \frac{w}{w_m}\right)\left(\frac{\partial^2 n}{\partial x^2}\right) - \mu_1 \frac{\partial n}{\partial x}\frac{\partial w}{\partial x} + B(n,w) - D(n,w) \tag{5.5}$$

$$\frac{\partial w}{\partial t} = \mu_1 \left(1 - \frac{w}{w_m}\right)\frac{1}{n}\left(\frac{\partial n}{\partial x}\right)\left(\frac{\partial w}{\partial x}\right) + \frac{B(n,w)}{n}(w_b - w) + G(n,w) \tag{5.6}$$

We consider a scenario where there is high birth rate (β), high initial density (n). We assume that the mass (w) is bounded below by birth mass (w_b) and bounded above by maximum mass (w_m).

Table 5.14: Parameters for Scenario 3

Parameters	Value
Transport rate (μ)	0.01
Maximum instantaneous per capita birth rate (β)	42
Mass dependent natural mortality (d)	$d(w)$
Minimum natural mortality (d_{min})	0.5
Miximum natural mortality (d_{max})	10
Maximum instantaneous per capita average growth rate(ψ)	1.5
Harvesting rate (f)	3.37
Birth mass (w_b)	0.01
Maximum mass (w_m)	0.2

The mass dependent natural mortality $d(w)$ in the above Table (5.14) is given by expression (5.3).

Table 5.15: Dimension less ratio of rates

Dimensional ratios	Value
$a = \frac{\frac{\mu}{Lm^2}}{\beta}$	0.0238
$b = \frac{d}{\beta}$	varies with w
$b_1 = \frac{d+f}{\beta}$	varies with w
$c = \frac{\psi}{\beta}$	0.0357

The non-trivial equilibrium points of equations (5.5) and (5.6) for density and mass are given by,

$$(n^*, w^*) = \left(\frac{1 - \frac{b}{w^*}}{w^*}, \frac{-(c - W_b) \pm \sqrt{(c - W_b^2) + 4c}}{2} \right). \tag{5.7}$$

Here dimensionless ratio b in the equilibrium value for density n^* takes two forms.

In the non-fishing domain, b takes the form b_n,

$$b_n = \frac{d(w)}{\beta}. \tag{5.8}$$

On the fishing domain, b takes the form b_f,

$$b_f = \frac{d(w) + f}{\beta}. \tag{5.9}$$

Also

$$c = \frac{\psi}{\beta}, \;\; W_b = \frac{w_b}{w_m}. \tag{5.10}$$

5.6.1 Numerical Results

Figure 5.31 shows how the density and mass varies in different time levels, for mass-dependent mortality and birth rates. Fishing pressure in the center $(3, 7)$ of the domain brings down the number of individuals in that area. The numerical value of density, goes down by 50% (for time units $T = 0$ to $T = 10$) this is due to the high mass-dependent natural mortality, during the period of time individuals are small in size. As time progresses, individuals grow in size and attain its maximum mass w_m, which is the asymptotic mass in the numerical results. For large time ($T = 100$), density and mass reach their asymptotic values.

Figure 5.32 shows how the density and mass vary with time under mass dependent mortality and constant birth rates. Fishing pressure in the center of the domain $(3, 7)$

brings down the density in that area. The numerical results are similar to the previous results of mass dependent mortality. Density goes down by 50% in the first 10 time units. It can also be observed from the figure 5.32, mass asymptotes faster, under constant birth rate.

One can observe from the figure 5.33 how the density and mass varies with time under constant mortality and mass dependent birth rates. Fishing pressure brings down the density in the center of the domain. The effect of constant mortality can be observed in the figure 5.33 by comparing density at $T = 10$ to the previous two cases (I, II) of mass dependent natural mortality models. A fewer individuals die when constant mortality rates are included. The speed at which mass reaches its asymptotic value under this case is slower than the previous two cases (I, II). At large time $T = 100$, density and mass reach their asymptotic values.

Now we compare how the mass dependent and constant per capita rates affect the instantaneous biomass yield of brown shrimp population. The numerical results for instantaneous biomass yield over time is given in figure 5.34. It can be observed from the Figure 5.34 that instantaneous biomass yield is different. The speed at which density and mass reaches its asymptotic value under (1) case III is slowest (mass independent mortality) and (2) case II is fastest (mass independent reproduction) (3) case I is moderate (mass dependent reproduction and mortality). In turn, this drives the system (5.5) and (5.6) to equilibrium at different speeds (Figures 5.31, 5.32, 5.33) and hence the instantaneous biomass yield Figure 5.34.

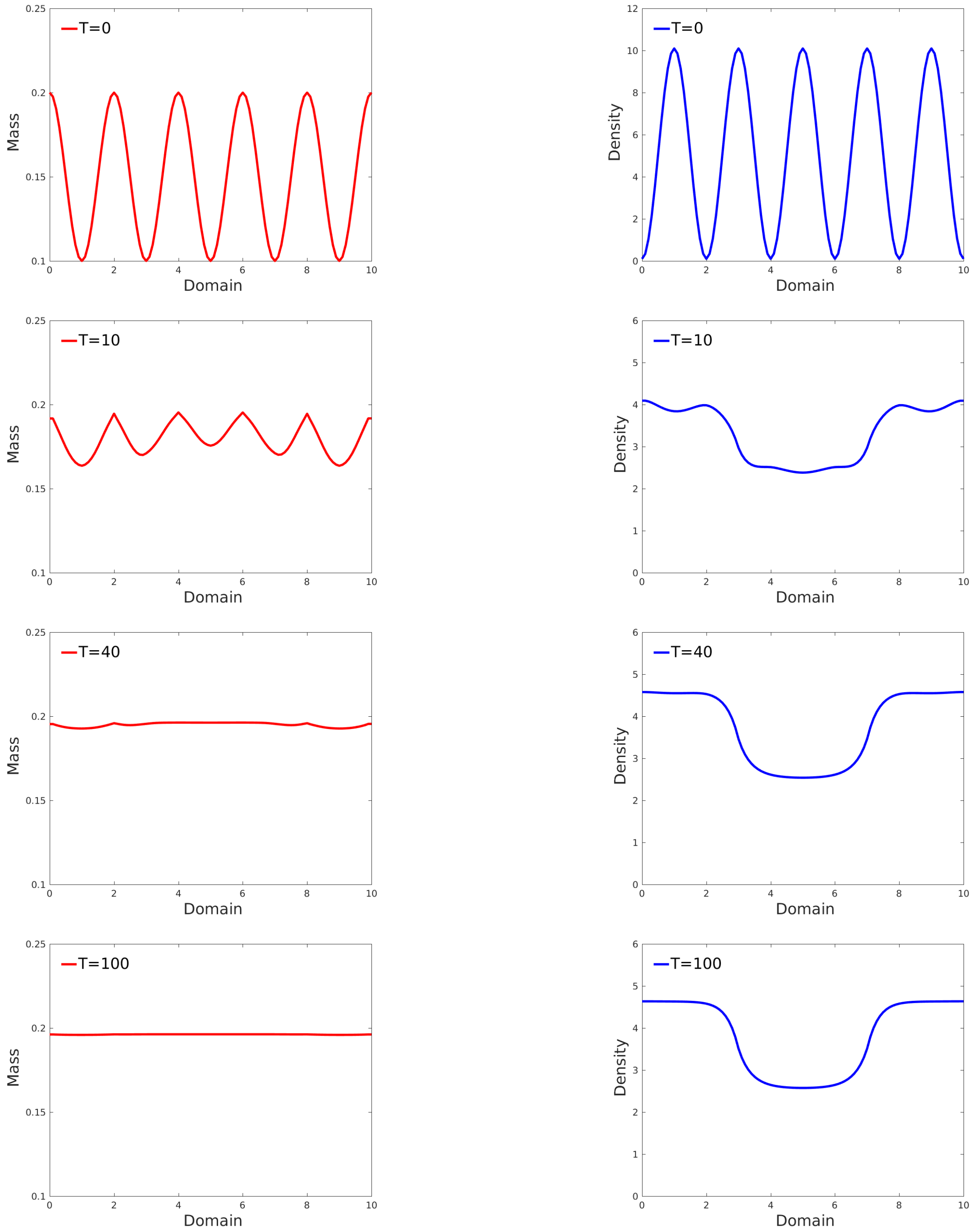

Figure 5.31: Mass dependent mortality and birth rates.

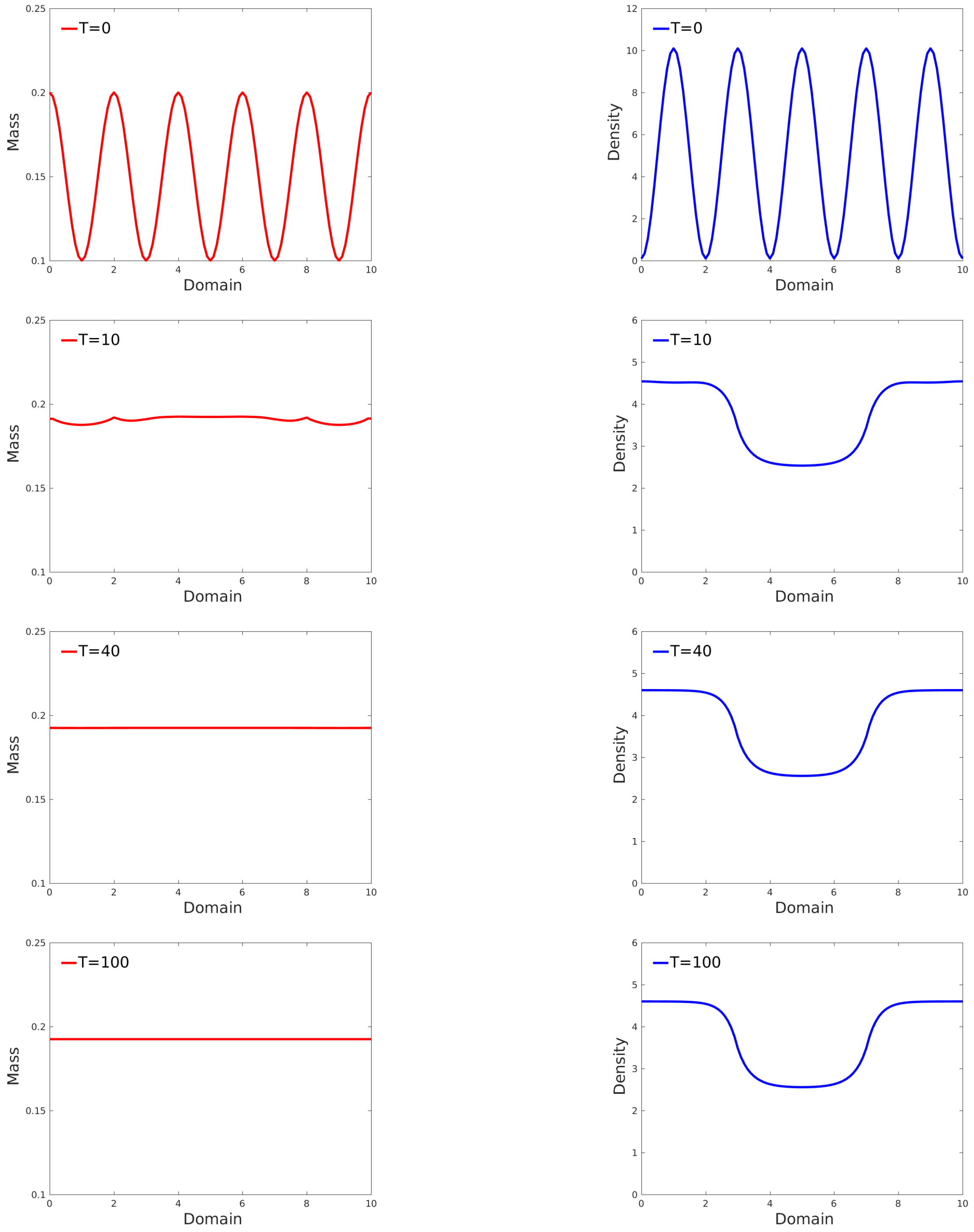

Figure 5.32: Mass dependent mortality and constant birth rates.

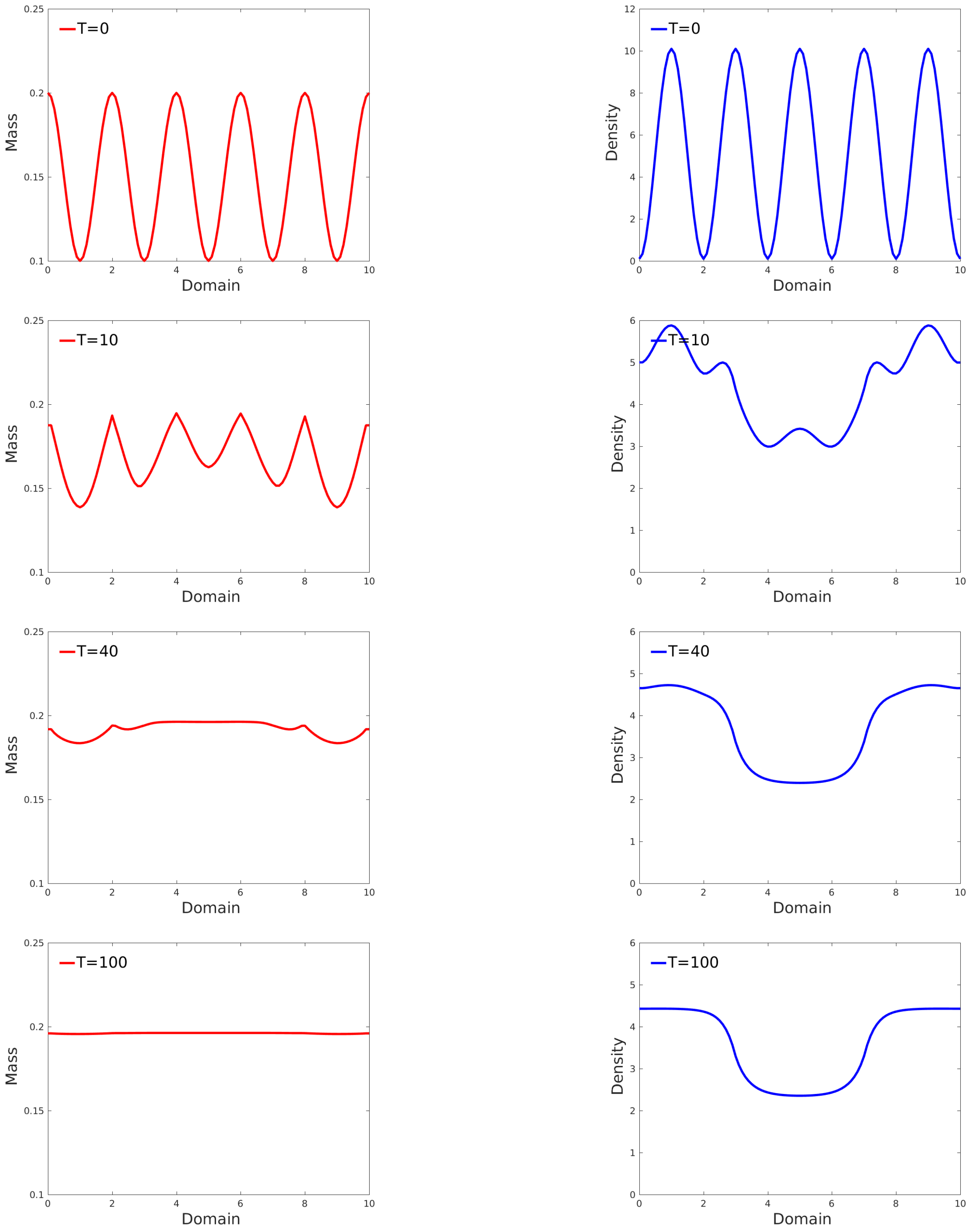

Figure 5.33: Constant mortality and mass dependent birth rates.

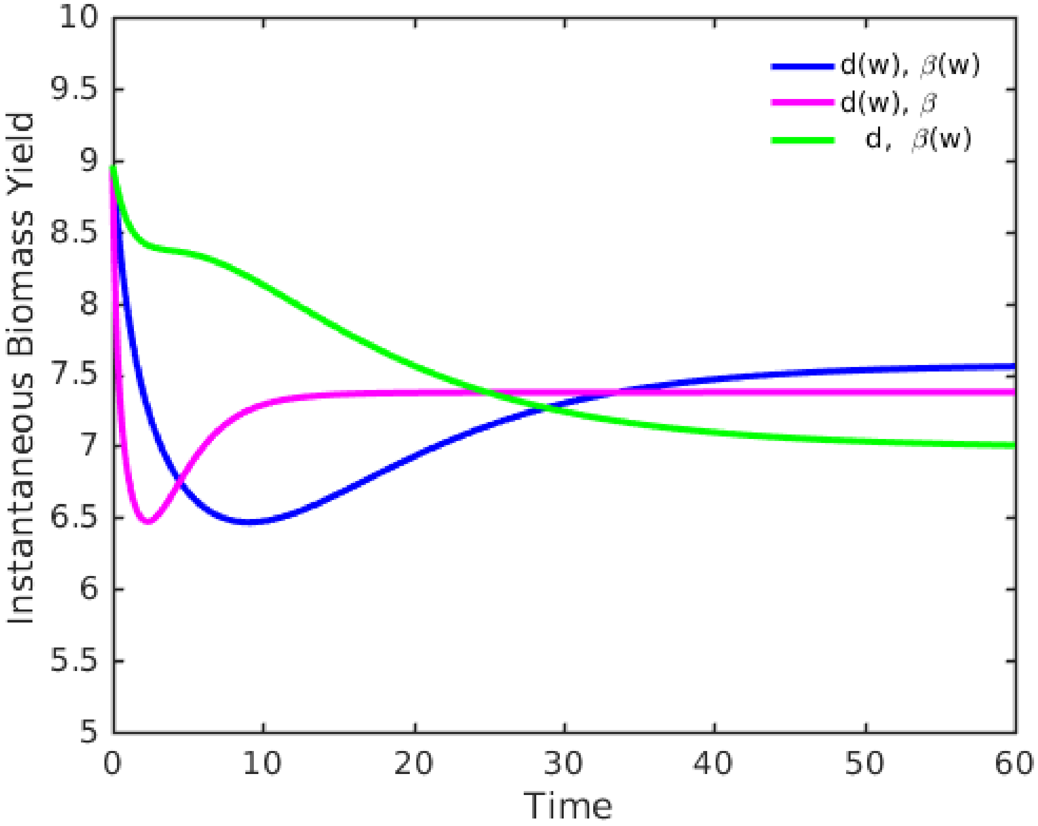

Figure 5.34: Instantaneous biomass yield for mass dependent/constant per capita rates versus time

To discuss the results for Scenario 3, we assume the actual answer to a problem is the numerical solution for mass dependent - mortality and birth, case I and compare this result with case II and case III, using the terms underestimate and overestimate.

When both mortality and birth are mass dependent, case I, instantaneous biomass yield continues to go down until large time $T = 10$. This is due to the mass dependent natural mortality $d(w)$. When the individuals are smaller they die with higher rate. During later period $T = 10$ to $T = 60$, instantaneous biomass yield increases due to mass dependent birth $\beta(w)$ because average mass becomes larger, and larger individuals produce more offspring which brings up the biomass. This in turn increases the instantaneous biomass yield.

An underestimate is an estimate that is lower than the actual answer to a problem. For the case II, when instantaneous birth rate β is constant, instantaneous biomass yield reaches the equilibrium faster and is underestimated because mass independent birth assumes mass does not affect per capita birth. This contradicts the example of Vermilion-rockfish in Chapter 1. An overestimate is an estimate that is greater than the actual answer to a problem. When natural mortality d is assumed to be a constant, case III, instantaneous biomass yield is monotonically decreasing function of time and is overestimated because mass independent death says individuals die at a constant rate, which contradicts the results from [1, 51].

Sustainable biomass yield is highest for case I, where both mortality and birth have mass dependency. It can be observed from the Figure 5.34, that instantaneous biomass yield goes down for case II at a faster rate than case I. The slower declining instantaneous biomass yield for case I (compared to case II) can be explained due to 1) higher body mass (mass dependent birth), and 2) lower mortality as body mass increases (mass dependent mortality).

The results from Scenario 3 suggest that mass independent per capita rates, either underestimate or overestimate the instantaneous biomass yield. So mass dependent per capita rates estimates the instantaneous biomass yield, more conservatively. So results from our model gives insights to mass dependent per capita rates, which are critically important for understanding the sustainability of a marine population.

6. CONCLUSION AND FUTURE WORK

6.1 Conclusion

This dissertation focussed on constructing a spatiotemporal population dynamics model to track density and average mass of a population at location x and at time t and apply it to a brown shrimp population in Gulf of Mexico. The system of equations resulting from our modeling approach, that is, coupled nonlinear reaction-diffusion equation and first-order nonlinear hyperbolic transport equation are quite complicated to analyze. There is very little known about its mathematical properties, if its inherited from reaction-diffusion equation or hyperbolic equation or if its behavior entirely different from either type. The spatially dependent coupled system of PDEs can have multiple solutions. The solutions of spatially homogeneous system were discussed in Chapter 3, which are indeed the equilibria for system of ODEs. Consequently, a finite difference scheme for the numerical solution to the system of coupled nonlinear PDEs was developed. In particular, key processes controlling populations like reproduction, growth, mortality and transport over various spatial and temporal scales were considered.

Three different diffusive transport rates (low, medium, high) were used to explore how the mobility of species from MPAs to fishing zone affects (1) the density and average mass of a population in and outside the protected areas and (2) instantaneous biomass yield and sustainable biomass yield in the fishing zone. High density gradient term was observed for low mobile species in the MPA due to (1) lower transport rate and (2) fewer number of individuals being transported from the MPA to the fishing zone. However a low density gradient term (for higher number of fishing zones) was observed in the scenario with high mobile species due to (1) high transport rate and

(2) a large number of individuals in MPAs being transported to the fishing zones.

The numerical results for instantaneous biomass yield suggests that when we establish a network of marine protected areas along a coastline, starting from two MPAs in one fishing zone scenario to fifteen MPAs in sixteen fishing zones scenario, instantaneous biomass yield is always higher for a species with high mobility when fishing with maximum sustainable fishing rate f_S. Sustainability was captured when the model was tested for wide range of fishing rates with multiple fishing zones and a network of MPAs. The numerical results suggest that, for a low mobile species, when 1) fishing rate is increased and 2) increasing the number of fishing zones, biomass yield becomes sustainable. However, for a medium and high mobile species, when fishing at higher fishing rates ($f > f_I$), biomass yield declines with increase in the fishing rate. So this suggests that there is a need to identify the mobility of species before MPA implementation.

Spatially explicit harvesting strategy was explored. Suppose that MSY for a spatially uniform distribution (ODE models) occur at the fishing rate f_S. When a spatially explicit harvesting strategies are considered, MSBY does not occur at f_S. The results shows that depending on the number of fishing zones, MSBY fishing rate is different. So this suggests that, when MPAs are introduced, the fishing rates should be adjusted to reach the MSBY. The numerical results shows population collapses for large number of fishing zones, fishing at higher fishing rates ($f > f_I$) , and high transport rate.

Mortality rates of marine organisms are different between different life stages [9]. It has also been demonstrated that as shrimp grows, there is low vulnerability of juveniles due to predation [51]. We investigated mass dependent mortality and reproduction and discussed how it affects density and mass. The numerical solutions show that sustainable biomass yield was high with mass dependent rates than mass independent rates. Thus results from our model suggest mass dependent per capita rates are critically important for understanding the sustainability of a marine population.

From the discussion of results, one can get a general understanding of how a network of MPAs affects fisheries harvests, but studies on how vital rates dynamics, birth, growth, mortality, transport are likely to increase or decrease the value of MPAs as a management tool is lacking [33]. New modeling approaches are insightful by predicting the fishing effort and designing network of MPAs and studying how these key factors can be used to balance population sustainability and yield.

6.2 Future Work

While this dissertation has demonstrated the use of creating 1D spatio-temporal population dynamics model, many opportunities for extending the scope of this dissertation remains open. This section presents some of these directions. By extending the present 1D model to a 2D model, one could investigate consistency and stability of the numerical scheme, estimate errors in numerical solutions using grid convergence technique. Other research directions would be to test the system of coupled PDEs for the existence of global attractor.

The present model can be used to study density and mass fluctuations with changes in the birth, death, growth transport rates for different fish populations. To test the utility of the model, one could compare the numerical results of the model with the field data available. It is interesting to study the model for different fish species by varying the transport rates and investigate sustainable biomass yield in multiple fishing zones when networks of MPAs have been established. The idea of dividing the coastal line into multiple fishing zones and creating a network of MPAs can be used to explore the competition model, that is, when two or more different species compete for resources.

REFERENCES

[1] J. T. Anderson, *A review of size dependent survival during pre-recruit stages of fishes in relation to recruitment,* J. Northwest Atl. Fish. Sci., Vol. 8 (1988).

[2] H.G. Andrewartha and L.C. Birch, *Distribution and abundance of animals*, University of Chicago Press, 1954.

[3] R. Baker, M. Fujiwara and T. J. Minello, *Juvenile growth and mortality effects on white shrimp Litopenaeus setiferus population dynamics in the northern Gulf of Mexico,* Fish. Res., 155 (2014), pp. 74-82.

[4] A. Bakun, *Definition of environmental variability affecting biological processes in large marine ecosystems,* In Variability and Management of Large Marine Ecosystems, ed. K. Sherman and L.M. Alexander, American Association for the Advancement of Science Selected Symposium 99, Westview Press, Boulder, Colorado, USA, (1986), pp. 89-108.

[5] L. Berezansky, L. Idels and M. Kipnis, *Mathematical model of marine protected area,* IMA J. Appl. Math., 76 (2) (2011), pp. 312-325.

[6] S. C. Burgess, K. J. Nickols, C. D. Griesemer, L. A. K. Barnett, A. G. Dedrick, E. V. Satterthwaite, L. Yamane, S G. Morgan, J. W. White, L. W. Botsford, *Beyond connectivity: how empirical methods can quantify population persistence to improve marine protected area design,* Ecol Appl., 24(2) (2014), pp. 257–270.

[7] H. Brezis and F. Browder, *Partial differential equations in the 20th century,* Adv. Math, 135 Article No. AI971713 (1998), pp. 76-144.

[8] S. K. Brown, P. J. Auster, L. Lauck, and M. Coyne, *Ecological effects of fishing,* NOAA's State of the Coast Report, Silver Spring, NOAA, 1998.

[9] J. F. Caddy, *Modelling natural mortality with age in short-lived invertebrate populations: definition of a strategy of gnomonic time division,* Aquat. Living Resour., 9 (1996), pp. 197-207.

[10] R. E. Crabtree, *Endangered species act-section 7 consultation biological opinion,* NOAA, NMFS, SERO, 2012.

[11] R. Gillett, *Global study of shrimp fisheries,* FAO Fisheries Technical Paper, No. 475, Rome, FAO, 2008.

[12] P. E. Carothers and W. E. Grant, *Fishery management implications of recruitment seasonality: simulation of the Texas fishery for the brown shrimp, Penaeus aztecus,* Ecol. Model., 36 (1987), pp. 239-268.

[13] H. Caspers, F. R. Harden Jones, *Fish migration,* Edward Arnold (Publishers) Ltd., London 1968.

[14] J. G. Charney, R. Fjørtoft, J. Von Neumann, *Numerical integration of the barotropic vorticity equation,* Tellus, 2 (1950), pp. 237–254.

[15] C. N. Christou and L. V. Idels, *Bioeconomical Ricker's model of marine protected areas,* Electron. J. of Differential Equations, Vol. 76 (2012), pp. 1–11 .

[16] R. Courant, K. O. Friedrichs and H. Lewy, *Über die partiellen differenzengleichungen der mathematischen physik.,* Math. Ann., 100 (1928), pp. 32–74. (English translation, with commentaries by P. B. Lax, O. B. Widlund, S.V. Parter, in IBM J. Res. Develop. 11 (1967).)

[17] J. Crank and P. Nicolson, *A practical method for numerical evaluation of solutions of partial differential equations of heat conduction type,* Proc. Camb. Phil. Soc., 43 (1947), pp. 50–67.

[18] NOAA Fisheries, Fishwatch U. S. Seafood Facts, URL `http://www.fishwatch.gov/profiles/brown-shrimp`.

[19] K. O. Friedrichs, *Symmetric hyperbolic linear differential equations,* Comm. Pure Appl. Math, 7 (1954), pp 345–392.

[20] S. A. Gerschgorin, *Error estimate for the finite difference method for solving partial differential equations,* J. Appl. Math. Mech., Volume 10, Issue 4, (1930), pp. 373-382.

[21] United States Gulf of Mexico fisheries information, URL `http://gulffishinfo.org/Species`.

[22] ICES, *Report of the ICES advisory committee,* ICES Advice, Book 1, 2012.

[23] N. J. Gotelli, *A primer of ecology*, 4th Edition, Sinauer Associates, 2009.

[24] T. G. Hallam and S. A. Levin, *Mathematical ecology: An introduction,* Biomathematics, Vol.17, Springer-Verlag, Berlin, 1986.

[25] T. D. Harwood, *The circular definition of populations and its implications for biological sampling,* Mol. Ecol., 18 (2009), pp. 765–768.

[26] D. A. Hart, *When do marine reserves increase fishery yield?,* Can. J. Fish. Aquat. Sci., 63 (2006), pp. 1445–1449.

[27] R. A. Hart, *Stock assessment update for brown shrimp, Farfantepenaeus aztecus in the U.S. Gulf of Mexico,* NOAA Fisheries, SEFC, Galveston Laboratory, 2012.

[28] R. A. Hart, *Stock assessment update for brown shrimp, Farfantepenaeus aztecus in the U.S. Gulf of Mexico,* NOAA Fisheries, SEFC, Galveston Laboratory, 2015.

[29] A. Hastings, L. W. Botsford, *Equivalence in yield from marine reserves and traditional fisheries management,* Science, 284 (1999), pp. 1537–1538.

[30] K. H. Hauge, B. Cleeland, and D. C. Wilson, *Fisheries depletion and collapse,* International Risk Governance Council (IRGC) Report, 2009.

[31] R. Hilborn, *Overfishing: What everyone needs to know,* Oxford University Press, Oxford, 2012.

[32] S. Jennings, M. J. Kaiser and J. D. Reynolds, *Marine fisheries ecology,* Blackwell Publishing, 2001.

[33] D. M. Kaplan, *Fish life histories and marine protected areas: an odd couple?,* Mar. Ecol. Prog. Ser., Vol. 377 (2009), pp. 213–225.

[34] B. L. Keyfitz and N. Keyfitz, *The McKendrick partial differential equation and its uses in epidemiology and population study,* Mathl. Comput. Modelling, Vol. 26, No. 6 (1997), pp. 1-9.

[35] C. C. Kohler and W. A. Hubert, *Inland fisheries management in North America,* 2nd edition, American Fisheries Society, 1999.

[36] A. N. Kolmogorov, I. G. Petrovsky and N. S. Piskunov, *Investigation of the equation of diffusion combined with increasing of the substance and its application to a biology problem,* Bull Moscow State Univ Ser A: Math and Mech, 1(6) (1937), pp. 1–26.

[37] M. Kot, *Elements of mathematical ecology*, Cambridge University Press, 2001.

[38] J. A. Koslow, G. W. Boehlert, J. D. M. Gordon, R. L. Haedrich, P. Lorance, and N. Parin, *Continental slope and deep-sea fisheries: implications for a fragile ecosystem,* ICES J. Mar. Sci., 57 (3) (2000), pp. 548-557.

[39] M. Lindegren, D. M. Checkley, T. Rouyer, A. D MacCall, and N. C. Stenseth, *Climate, fishing, and fluctuations of sardine and anchovy in the California Cur-*

rent, Proceedings of the National Academy of Sciences of the United States of America, 110(33), 13672–13677, 2013.

[40] C. J. Krebs, *Ecology: The experimental analysis of distribution and abundance*, Second Edition, Harper and Row, New York, 1978.

[41] Laguna Bluebelt Coalition, *Marine Reserves,* URL `http://lagunabluebelt.org`.

[42] D. R. Lassuy. *Species profiles: life histories and environmental requirements (Gulf of Mexico): brown shrimp,* U. S. Fish Wildl. Serv., Biol. Serv. Prog. FWS/OBS 82/11.1 (1983).

[43] P. D. Lax, R. D. Richtmyer, *Survey of the stability of linear finite difference equations,* Comm. Pure Appl. Math., 9 (1956), pp.267-293.

[44] P. D. Lax, *On the stability of difference approximations to solutions of hyperbolic differential equations,* Comm. Pure Appl. Math., 14 (1961), pp. 497–520.

[45] W. H. Lear, *History of fisheries in the Northwest Atlantic: the 500-year perspective,* J. Northwest Atl. Fish. Sci., 23 (1998), pp. 41-74.

[46] G. A. De Leo , F. Micheli, *The good, the bad and the ugly of marine reserves for fishery yields,* Phil. Trans. R. Soc. B, 370: 20140276, (2015).

[47] J. Lubchenco, S. R. Palumbi, S. D. Gaines, and S. Andelmans, *Plugging a hole in the ocean: The emerging science of marine reserves,* Ecol. Appl., Volume: 13 Issue: 1 (2003), pp. S3-S7.

[48] M. S. Love, P. Morris, M. McCrae, R. Collins, *Life history aspects of 19 rockfish species (Scorpaenidae: Sebastes) from the Southern California Bight,* NOAA Technical Report, NMFS 87, (1990).

[49] Marine Parks Authority, *A review of benefits of marine protected areas and related zoning considerations,* 2008.

[50] Analysis of United States MPAs, *National MPA center's MPA Inventory,* 2012.

[51] T. J. Minello, R. J. Zimmerman and E. X. Martinez, *Mortality of young brown shrimp (Penaeus azetecus) in estuarine nurseries,* Trans. Am. Fish. Soc., 118 (1989), pp. 693-708.

[52] T. J. Minello and R. J. Zimmerman, *First predation of juvenile brown shrimp (Penaeus azetecus) Ives: the effects of simulated Spartina structure on predation rates,* J. Exp. Mar. Biol. Ecol., 72 (1983), pp. 211-231.

[53] S. A. Murawski, *Rebuilding depleted fish stocks: the good, the bad, and, mostly, the ugly,* ICES J. Mar. Sci., 67 (9) (2010).

[54] J. D. Murray, *Mathematical biology,* Springer, Second Edition, 1993.

[55] S. N. Murray, R. Ambrose, J. Bohnsack, L. Botsford, M. Carr, G. Davis, P. Dayton, D. Gotshall, D. Gunderson, M. Hixon, J. Lubchenco, M. Mangel, A. MacCall, D. McArdle, J. Ogden, J. Roughgarden, R. Starr, M. Tegner, and M. Yoklavich, *No-take reserve networks: Sustaining fishery populations and marine ecosystems,* Fisheries, Vol.24, No.11, (1999), pp. 11-25.

[56] R. A. Myers, J. A. Hutchings and N. J. Barrowman, *Why do fish stocks collapse? The example of Cod in Atlantic Canada,* Ecol. Appl., Vol. 7, No. 1, (1997), pp. 91-106.

[57] M. G. Neubert, *Marine reserves and optimal harvesting,* Ecol. Lett., 6 (2003), pp. 843–849.

[58] J. M. Nance, E. F. Klima and T. E. Czapla, *Gulf of Mexico shrimp stock assessment workshop,* NOAA Technical Memorandum, NMFS-SEFC-239, 1989.

[59] R. M. Nisbet and W.S.C. Gurney, *Modelling fluctuating populations,* John Wiley & Sons, 1982.

[60] Q. T. K. NGOC, *Marine Protected Areas: A review on their benefits and designs for fisheries management,* Asian Fish. Sci., 27 (2014), pp.185-198.

[61] National Marine Protected Areas Center, *Framework for the National System of Marine Protected Areas of the United States of America,* URL `marineprotectedareas.noaa.gov`.

[62] NOAA, National Oceanic & Atmospheric administration, URL `http://oceanservice.noaa.gov/ecosystems/mpa/`.

[63] NOAA fisheries glossary, *NOAA technical memorandum NMFS-F/SPO-69,* Revised Edition, June 2006.

[64] NRC research press, *Report on Johan Hjort symposium on recruitment dynamics and stock variability*, 2016.

[65] D. Pauly, V. Christensen, S. Guénette, T. J. Pitcher, U. Rashid Sumaila, C. J. Walters, R. Watson and D. Zeller, *Towards sustainability in world fisheries,* Nature, 418 (2002), pp. 689-695.

[66] PFMC, The Pacific Fishery Management Council, URL `http://www.pcouncil.org/habitat-and-communities/marine-protected-areas/`.

[67] D. W. Peaceman and H. H. Rachford Jr., *The numerical solution of parabolic and elliptic differential equations,* J. Soc. Indust. Appl. Math., 3 (1955), pp. 28-41.

[68] J. C. V. Pezzey, C. M. Roberts, B. T. Urdal, *A simple bioeconomic model of a marine reserve,* Ecol. Econ., 33 (2000), pp. 77–91.

[69] R. J. LeVeque, *Finite difference methods for ordinary and partial differential equations: Steady-state and time-dependent problems,* SIAM, 2007.

[70] R. K. Wallace, K. Fletcher, *Understanding fisheries management,* Auburn University and the University of Mississippi, the Auburn University Marine Extension and Research Center, the Mississippi Alabama Sea Grant Legal Program, and the Mississippi Law Research, Second Edition, 1996.

[71] C. M. Roberts, and J. P. Hawkins, *How small can a marine reserve be and still be effective?* Coral Reefs, 16:150 (1997).

[72] J. N. Sanchirico, *Marine Protected Areas as fishery policy: A discussion of potential costs and benefits,* Resources for the Future, 00-23, 2000.

[73] J. N. Sanchirico, and J. E. Wilen, *A Bioeconomic model of marine reserve creation,* J. Environ. Econ. Manage., 42 (2001), pp.257-276.

[74] V. K. Saulev, *On a class of elliptic equations solvable by the method of finite differences,* Vycisl. Mat., 1 (1957), pp. 81–86.

[75] P. Sparre, S. C. Venema, *Introduction to tropical fish stock assessment - Part 1, Manual,* FAO Fisheries Technical Paper. No. 306.1, Rev. 2., Rome, FAO, 1998.

[76] R. W. Sterner, G. E. Small and J. M. Hood, *The conservation of mass,* Nature Education Knowledge, 3 (2011).

[77] J. C. Strikwerda, and B. A. Wade, *A survey of the Kreiss matrix theorem for power bounded families of matrices and its extensions,* Banach Center Publ., 38 (1997), pp. 339-360 .

[78] J. C. Strikwerda, *Finite difference schemes and partial differential equations,,* SIAM, 2004.

[79] A. Temming, M. Hufnagl, *Decreasing predation levels and increasing landings challenge the paradigm of non-management of North Sea brown shrimp (Crangon crangon),* ICES J. Mar. Sci., 72 (3) (2014), pp. 804-823.

[80] TPWD News, News Release, Media Contact: news@tpwd.texas.gov, URL `http://tpwd.texas.gov/newsmedia/releases/?req=20160505a&nrtype=all&nrspan=2016&nrsearch=shrimp`, May 5, (2016).

[81] V. Thomée, *From finite differences to finite elements: A short history of numerical analysis of partial differential equations,* J. Comput. Appl. Math., Volume 128, Issues 1–2, (2001), pp. 1–54.

[82] P. Turchin, *Does population ecology have general laws?,* Oikos Volume 94, (2001), pp. 17–26.

[83] C. Walters, *Impacts of dispersal, ecological interactions, and fishing effort dynamics on efficacy of marine protected areas: how large should protected areas be?* Bull. Mar. Sci., 66.3 (2000), pp. 745-757.

[84] J. R. Walton, *Lecture notes on Modeling spatial effects,* Lecture notes for Math 469, Spring 2012, Texas A&M University.

[85] B. Wendroff, *On central difference equations for hyperbolic systems,* J. Soc. Indust. Appl. Math., 8 (1960) pp. 549–555.

[86] Young People's Trust for the environment YTPE, *Overfishing fact sheet,* URL `http://ypte.org.uk/factsheets/overfishing/introduction`.